2012

Anomalous Wave Dispersion in the Cyclohexanedione-Bromate Chemical Oscillator

Ryan Boger
The University of Montana

ANOMALOUS WAVE DISPERSION IN THE CYCLOHEXANEDIONE-BROMATE CHEMICAL OSCILLATOR

By

Ryan Michael Boger

B.S. Chemistry, The University of Notre Dame, South Bend, IN, 2001

Dissertation

presented in partial fulfillment of the requirements
for the degree of

Ph.D.
in Chemistry

The University of Montana
Missoula, MT

December, 2011

Approved by:

Sandy Ross, Associate Dean of The Graduate School
Graduate School

Richard J. Field, Chair
Chemistry and Biochemistry

Michael DeGrandpre
Chemistry and Biochemistry

Donald Kiely
Chemistry and Biochemistry

Robert Yokelson
Chemistry and Biochemistry

Jesse Johnson
Computer Science

Boger, Ryan, Ph.D., Fall 2011 Chemistry

Anomalous Wave-Velocity Dispersion in the Ferroin-Catalyzed CHD-BZ Chemical Oscillator

Chairperson: Professor Richard J. Field

A modified six-variable Oregonator model presented here successfully reproduces a significant portion of the behavior observed in the Ferroin-catalyzed cyclohexanedione variant of the Belousov-Zhabotinsky (CHD-BZ) reaction. The phenomena of anomalous velocity dispersion (in which following waves may catch up to, rather than fall behind an initial excitation wave), wave-stacking, and backfiring have been successfully reproduced numerically as resulting from non-monotonic [Br^-] decay to the steady state in the wake of an excitation pulse. The non-monotonic decay is seen as a "dip" in [Br^-] following the passage of a chemical wave. This dip in [Br^-] decay curve allows a following wave to accelerate and catch up to the initial wave. The origin of anomalous dispersion as the result of such a non-monotonic decay curve in [Br^-] has been suggested previously by Steinbock et al. and Szalai et al. However, the work presented here is the first successful representation of anomalous wave-velocity dispersion using a chemical model. This model is based on the well-understood chemistry of the Oregonator model of the Belousov-Zhabotinsky reaction, coupled to a second pathway (based on chemistry related to uncatalyzed bromate oscillators) for the oxidation of organic substrate to provide the new dynamics.

Contents

List of Figures

List of Tables

1 INTRODUCTION.

We provide here an introduction to general ideas of far-from-equilibrium chemical dynamics as well as general considerations of the chemistry and dynamics of oscillating chemical reactions and traveling waves. The concept of anomalous dispersion in a set of traveling waves is introduced. The chemistry and dynamics of the oscillatory Belousov-Zhabotinsky (BZ) reaction in both its metal-ion catalyzed and uncatalyzed variations is discussed in detail, and its reduction to the simple Oregonator model is considered.

1.1 Thermodynamic Factors

This work involves dynamic phenomena displayed by complex reacting chemical systems (Field (2008)), whose behavior may be rationalized by means of a mechanism composed of some number of simple chemical reactions, typically assumed to be elementary, i.e., occurring in a single collision (Espenson (1995); Houston (2001)). Such simple reactions are often represented by the general reaction $a\mathrm{A} + b\mathrm{B} \rightarrow c\mathrm{C} + d\mathrm{D}$. Lower-case letters in the preceding equation refer to stoichiometric coefficients, and upper-case letters refer to chemical species (Field (2008); Atkins and de Paula (2009)). The rates of these reactions are, according to the Law of Mass Action (Field (2008)), in most cases proportional to the concentration of a single reacting chemical species, e.g., Rate $= (1/c)\mathrm{d[C]}/d\mathrm{t} = k\mathrm{[A]}$, that is, linear dynamics, or proportional to the concentrations of two (either reactant or product) species, e.g., Rate $= (1/d)d\mathrm{[D]}/d\mathrm{t}$

= (k)[A][D], i.e., nonlinear (in this case also autocatalytic) (Epstein and Pojman (1998)) dynamics. The parameter k is the rate constant for the particular chemical reaction represented.

The most interesting behaviors of such complex chemical systems occur far from thermodynamic equilibrium and are governed by overall dynamic laws containing positive and/or negative feedback loops (Nicolis et al. (1975); Nicolis and Prigogine (1977, 1989)).

1.1.1 Thermodynamic and Kinetic Constraints at or Near to Chemical Equilibrium

The state of chemical equilibrium (Pitzer (1995)) is very special. It is a dynamic state in which individual atoms and molecules are in a continual process of interconversion via individual elementary reactions among species identified as reactants, products and intermediates. However, the net rates of production and consumption of all species at the equilibrium state are balanced and no net chemical change occurs. Furthermore, the principle of detailed balance (based on the time-reversibility of wave mechanics) requires that at chemical equilibrium each elementary process at equilibrium must proceed at the same rate in both the forward and the reverse direction (Steinfeld et al. (1999); Houston (2001)). A chemical system not at thermodynamic equilibrium (Pitzer (1995)) will spontaneously move toward equilibrium. This change will be accompanied by an increase in entropy ($\Delta S > 0$). At equilibrium $\Delta S = 0$ and S is a maximum. It is also true that during spontaneous motion toward chemical equilibrium $\Delta G = \Delta H$ - $T\Delta S < 0$, reaching a minimum at equilibrium. At the point of chemical equilibrium (starting from a particular set of initial concentrations) the

thermodynamic requirement $\Delta G = 0$ (G is a minimum) requires the system to take on a unique chemical composition! The above constraints cause the behavior of chemical systems at or near to equilibrium to be relatively simple. Thus the behavior of chemical systems is not complex compared to mechanical systems. For example, the principle of detailed balance requires they cannot approach their equilibrium point via damped oscillation (about it) as can a pendulum. Isolated chemical systems closed to the exchange of matter with their environment must approach their final equilibrium composition monotonically. Neither damped nor undamped oscillations of chemical concentrations are possible near to chemical equilibrium.

This restriction to monotonic motion does not hold far-from-equilibrium (Prigogine and Nicolis (1967); Nicolis and Prigogine (1977, 1989)) even in systems closed to exchange of matter! Chemical driving forces may become very large and nonlinear in a system far-from-equilibrium, and detailed balance is no longer maintained. Thermodynamics gives us no guidance to behavior during the early stages of reaction in an initially far-from-equilibrium system. Furthermore, nearly all thermodynamic bets are off in a system open to exchange of matter as well as energy with its environment. In such cases we may see both thermodynamically spontaneous behaviors and behaviors driven by matter or energy exchange. Spontaneous changes must still be accompanied by decreasing ΔG. Far-from-equilibrium chemical phenomena we will investigate here include oscillation of the concentrations of intermediate species and reaction-diffusion supported moving or stationary patterns of intermediate concentrations (Epstein and Pojman (1998)). Oscillations and spatial patterns are often observed in the same chemical system. Some initial considerations concerning the thermodynamic constraints on oscillating chemical reactions can be made and are

important. The most significant constraint is that in a closed system the concentrations of only intermediate species may oscillate. The decrease in free energy necessary to drive the oscillations must result from the spontaneous monotonic disappearance of some species referred to as reactants and appearance of other species referred to as products, $\Delta G_{overall} < 0$. The concentrations of reactant species must be much higher than the concentrations of oscillatory intermediates in order to sustain a far-from-equilibrium condition. Furthermore, no particular elementary reaction can proceed in the forward direction during one stage of the overall approach to equilibrium and in the reverse direction in another stage.

We point out the existence of dynamic stationary states of the concentration of intermediate species during an oscillating, or any other, chemical reaction. These states are thought by some to be characterized by a minimum entropy production associated with the set of elementary reactions involved in the stationary state (Prigogine and Nicolis (1967)). Steady states may be stable or unstable.

1.2 Oscillating Chemical Reactions - History

1.2.1 Temporal Oscillation

Oscillation of intermediate species concentrations in the biochemistry of living cells has been occurring since the beginning of life on earth, especially in metabolic processes. However, the systematic investigation of oscillating enzyme reactions (and other oscillations) found in living organisms (Tyson et al. (1989); Winfree (2002)) and oscillations in non-biological organic and inorganic chemical systems, as well as development of the theory of dynamic far-from-equilibrium systems is a relatively recent endeavor (Epstein and Pojman (1998)). Indeed serious systematic work in this

area became established only in the 1960s and 70s.

The earliest mention of an oscillating chemical reaction appears to be the report by Robert Boyle (Boyle (1680)) of emission of periodic pulses of light during the gas-phase oxidation of phosphorus. Early reports of oscillation in non-homogeneous (multi-phasic) systems include the oscillation of current in an electrochemical system by Fechner (Fechner (1828)) and oscillation in the rate of chromium oxidation in aqueous acid by Ostwald (Ostwald (1899)). Special mention also is due early pioneering experimental work and theoretical interpretation by W.C. Bray(Bray (1921)), Bray and Caulkins (Bray and Caulkins (1931)), Bray and Liebhafsky (Bray and Liebhafsky (1931)), and Liebhafsky, Furuichi, and Roe (Liebhafsky et al. (1981)) of oscillation of $[I_2]$ during the IO_3^--catalyzed decomposition of H_2O_2 and the later systematic investigation of oscillatory, gas-phase combustion chemistry by Peter Gray and colleagues (Gray et al. (1991)).

1.2.2 Modern History

The rapid growth of research work in oscillatory chemistry in the 1960s - 70s mentioned above resulted from the confluence of several factors, including a sense of theoretical legitimacy given to chemical oscillations in the 1960s by the theoretical work of Ilya Prigogine and coworkers (Nicolis and Prigogine (1977); Prigogine and Nicolis (1967)) on nonlinear, far-from-equilibrium chemical dynamics. This work led to understanding of so-called "dissipative structures" in which patterns in time and space may be supported by the dissipation of free energy. The above theoretical suggestions were supported by the nearly simultaneous discovery of an apparent experimental example of a Prigogine-like system by B.P. Belousov (Belousov (1958, 1982)) and its initial investigation and interpretation by A. M. Zhabotinsky(Zhabotinsky

(1991)). This system became known as the Belousov-Zhabotinsky (BZ) Reaction. It may generally be described as the metal-ion, e.g., (Ce(IV)/Ce(III) or $Fe(phen)_3^{3+}$ / $Fe(phen)_3^{2+}$-catalyzed (phen $\equiv$ 1,10-phenanthroline)) oxidation of organic substrates, e.g., $CH_2(COOH)_2$ or cyclohexanedione (CHD) by bromate (BrO_3^-) ion in strongly acid, aqueous media. The oscillations appear to result from an autocatalytic process generating $HBrO_2$ but subject to a negative feedback carried by Br^- (Zhabotinsky (1991)). Subsequent detailed elucidation of the fundamental mechanistic chemistry and dynamic structure of the so-called Belousov-Zhabotinsky (BZ) reaction by Field, Körös, and Noyes (FKN) in 1972 (Field et al. (1972)), and the suggestion by Field and Noyes (Field and Noyes (1974a)) of a skeleton chemical model (referred to as the Oregonator) that established the BZ chemistry as an example of a far-from-equilibrium system governed by a nonlinear dynamic law. Thus further exploration of the dynamics of oscillating chemical reactions, especially but not limited to the BZ system, became a heuristic method for understanding features of the mathematics of nonlinear dynamical systems, e.g., the Hopf bifurcation bistabiliy, oscillation, and chaos (Epstein and Pojman (1998); Strogatz (2001)). These efforts have drawn general interest from areas as diverse as mathematics, physics and biology.

Research in these areas came to fruition in the 1980s as a major area of interest, largely by the remarkably broad body of research on other (mostly inorganic) oscillating chemical reactions and basic ideas of nonlinear dynamics by I.R. Epstein, Ken Kustin and their colleagues at Brandeis University (Epstein and Pojman (1998)), coupled with their scientific and personal leadership.

1.2.3 Spatial Patterns

Zaikin and Zhabotinsky (Zaikin and Zhabotinskii (1970)) discovered traveling waves of chemical oxidation in the BZ reaction with $Fe(phen)_3^{3+}$(blue)/$Fe(phen)_3^{2+}$(red) as catalyst and $CH_2(COOH)_2$ as organic substrate. The liquid chemical reagent is spread in a thin-layer on a flat surface where the patterns appear as blue bands (ferriin) moving in a red (ferroin) medium. These nerve-impulse-like traveling waves (Field and Troy (1979)) result from coupling of an autocatalytic pulse in the FKN chemistry with diffusion of the autocatalytic species $HBrO_2$. Such chemical structures often appear as moving concentric circles centered on a so-called initiation pacemaker, whose mechanism of action is not yet fully understood (Hastings et al. (2003)). A.T Winfree (Winfree (1972)) soon showed that when a band is suitably broken, blue spirals develop and that these traveling bands of chemical activity are of considerable interest to biological structure and function, e.g., spatial structure development and signal transmission (Winfree (2002)).

The concentric moving bands described above often form a target-like pattern of concentric circles as shown in Figure 1.

Pacemakers may trigger circles at fairly rapid frequencies. Thus one circle may appear before its predecessor has moved far from the pacemaker center, causing it to follow the leading circle quite closely but to move more slowly because of increased (but declining with separation) $[Br^-]$ behind the leading circle. See FKN mechanism below for the source of Br^-. In such a case the following circle falls behind its predecessor while its speed increases as $[Br^-]$ decreases, eventually reaching the speed of its predecessor. Thus, far enough from the pacemaker center the circles are dispersed into a pattern of equally spaced circles moving at the same speed. This is referred to

Figure 1: Target Patterns in a Thin-layer of BZ Reagent in a 9-cm Diameter Petri Dish
(a) 1 minute after mixing; (b) after 3 min 30s; (c) after 7 min 15 s; (d) after 7 min 35 s; (e) after 16 min 20s. Three random pacemaker centers initiate targets, but as the system evolves, the successive annihilations of colliding waves from adjacent targets occur closer and closer to the lower frequency pacemaker. In time, the higher frequency source entrains the lower frequency one. In a given target pattern, the outermost wave travels at a slightly higher velocity than those inside the pattern. (Photographs by M. Pearson). From S.K. Scott, *Oscillations, Waves, and Chaos in Chemical Kinetics*, Oxford Science Publishers, Oxford.

Figure 2: Four Consecutive Snapshots of a Typical Target Pattern Showing Anomalous Wave-velocity Dispersion in the Ferroin-CHD-BZ Reaction

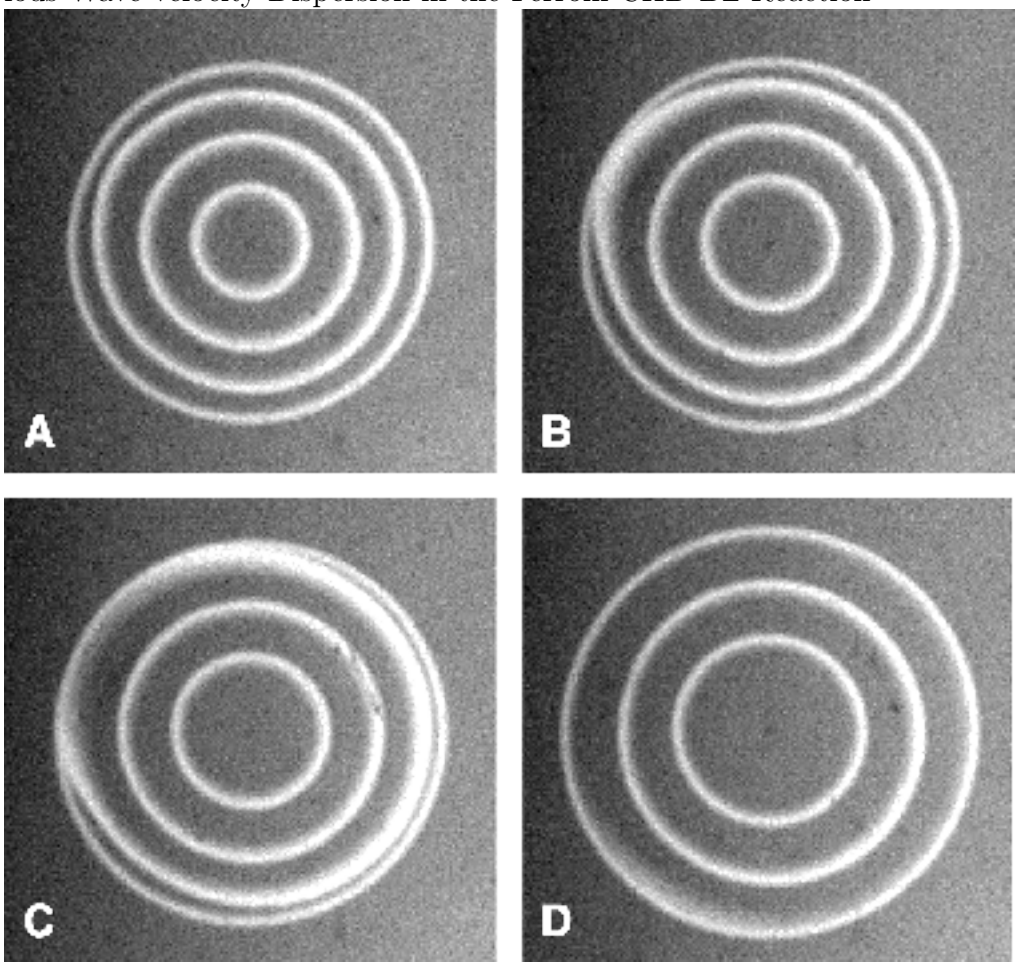

Time between snapshots: 10 s. Image size: 13.8 × 13.0 mm^2. Initial concentrations: [$NaBrO_3$] = 0.09 M, [1,4-CHD] = 0.19 M, [H_2SO_4] = 2.0 M, [ferroin] = 5.0 mM. Figure from Hamik and Steinbock (2003)

as “normal dispersion”.

Steinbock and coworkers (Hamik and Steinbock (2003); Manz and Steinbock (2004); Manz et al. (2006); Bordyugov et al. (2010)) discovered several years ago a BZ traveling-wave behavior he referred to as “anomalous dispersion”. A quasi two-dimensional experiment performed by Steinbock and co-workers (Hamik and Steinbock (2003)) shows anomalous dispersion in the concentric rings of a target pattern (fig. 2). The target pattern becomes non-concentric as waves accelerate and merge. Quasi one-dimensional experiments carried out in a 6-mm capillary tube containing a $Fe(phen)_3^{3+}/Fe(phen)_3^{2+}$-catalyzed BZ reagent with cyclohexanedione as the organic substrate and open to the atmosphere at one end show the anomalous phenomenon. It seems the atmosphere itself and/or some imperfection near the cut end of the glass capillary tube acts as a pacemaker. Thus moving bands of chemical activity are initiated near the end of the capillary and move down the cylinder of reagent. The anomalous behavior appears in several forms, apparently depending on the frequency of the pacemaker and the chemical composition of the reaction medium. Recall that “normal dispersion” at relatively rapid pacemaker-frequency is for successive bands to fall behind each other and speed up to eventually develop far from the pacemaker into a sequence of equally spaced bands traveling at the speed the first band moves into the steady state reagent. However, in an anomalous system, initially closely spaced bands may instead catch up with the one ahead of it, eventually reaching the same speed as this band or merging with it. Less closely spaced bands (slower pacemaker) tend to behave normally. In fact the range of observed anomalous behaviors includes densely packed patterns, well-segregated clusters, traveling shock structures, as well

the merging and stacking of waves discussed above (Vanag and Epstein (2001, 2002); Yang et al. (2002); Huh et al. (2001)).

The cyclohexanedione organic substrate used in the Steinbock anomalous dispersion system belongs to a class of organic BZ substrates, also including phenol and hydroxyquinone, which oscillate without a metal-ion catalyst. Only bromate ion and the substrate in an acidic medium is necessary for oscillation to occur. In this work we attempt to interpret anomalous dispersion as resulting from the coupling of the chemistries of a $Fe(phen)_3^{3+}/Fe(phen)_3^{2+}$-catalyzed cyclohexanedione oscillator and an uncatalyzed cyclohexanedione oscillator.

1.3 The Belousov-Zhabotinsky Reaction and the FKN Mechanism.

1.3.1 Classic Metal-Ion-Catalyzed Oscillations.

The BZ reaction is normally run in either a closed-system, batch reactor or an open Continuous-flow, Stirred Tank Reactor (CSTR) (Roux et al. (1983); Maselko and Swinney (1986); Gyorgyi et al. (1992)). Typical BZ initial concentrations (near to room temperature, 25 °C) in a batch reactor are $[BrO_3^-]_0 = 6.25\text{x}10^{-2}$ M, $[CH_2(COOH)_2]_0$ = 0.275 M, $[Ce(IV)]_0 = 2\text{x}10^{-3}$ M, and $[H^+]_0 = 2$ M (Scott (1994)). The reaction mixture must be well-stirred to avoid transient transport effects (Gyorgyi and Field (1992)). The system may be readily monitored electrochemically with a Pt-electrode sensitive to overall redox potential (typically controlled by [Ce(IV)]/[Ce(III)]) or a Br^-- selective electrode, both relative to a double-junction calomel electrode. Spectrophotometric methods may be used to measure metal-ion concentrations, e.g.,

Ce(IV) or $Fe(phen)_3^{3+}$, as well as the concentrations of other intermediate species including Br_2, HOBr, $BrO^{\bullet}_2$ or $HBrO_2$. Figure 3 shows typical BZ redox potential curves related to [Ce(IV)]/[Ce(III)] and ln $[Br^-]$.

Figure 3: Potentiometric Traces of ln $[Br^-]$ and ln [Ce(IV)]/[Ce(III)] for a Representative Belousov-Zhabotinsky Reaction

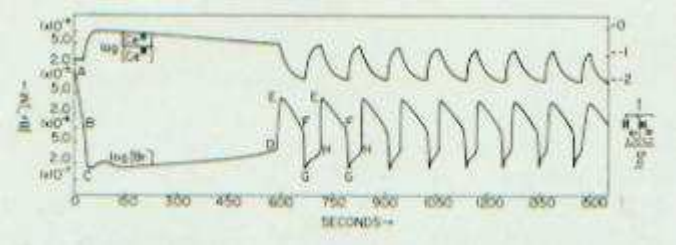

Initial concentrations: $[CH_2(COOH)_2]_0$ = 0.032 M; $[KBrO_3]_0$ = 0.063 M; $[KBr]_0$ = 1.5x10^{-5} M; $[Ce(NH_4)_2\ (NO_3)_5]_0$ = 0.001 M, $[H_2SO_4]_0$ = 0.8 M. From R.J. Field, E. Körös, and R.M. Noyes, *J. Amer. Chem. Soc.*, **1972** *94*, 8649- 8664.

Belousov-Zhabotinsky oscillations are typically preceded by an induction period (See Figure 3) after which oscillations appear at full amplitude rather than grow in from zero-amplitude. This is the behavior expected if the onset of oscillation is marked by a sub-critical Hopf bifurcation (Epstein and Pojman (1998); Strogatz (2001)). The amplitude of the oscillations change (increase or decrease) as the reaction proceeds, presumably because reactant concentrations decrease or product concentrations increase. True unchanging stationary states, completely periodic oscillatory states, or true chaotic states may be obtained, controlled and studied in a CSTR (Gyorgyi et al. (1992)).

Field, Körös, and Noyes (FKN) (Field et al. (1972)) suggested a chemical mechanism for occurrence of the BZ oscillations in the [Ce(IV)]/[Ce(III)]-catalyzed system with the organic substrate $CH_2(COOH)_2$. Their approach involves a pair of independent reaction sets coupled by a negative feedback loop. The first set (referred

to as Process A) occurs at high [Br^-] with the major effect of removal of [Br^-] to eventually yield $BrCH(COOH)_2$. The second set (referred to as Process B) occurs autocatalytically at [Br^-] below a critical value. Processes A and B are coupled by a third set of reactions (referred to as Process C) that generates Br^- when Process B is occurring at low [Br^-], thus supplying a strong negative feedback on Process B ($HBrO_2$, the autocatyalytic species in Process B is removed by Br^- in reaction R2 below) and shifting control of the system back to Process A as Process B slows down. Process A then begins the removal of Br^- to reset the cycle. The autocatalytic nature of Process B (carried by the intermediate $HBrO_2$) below a critical [Br^-] is important because it helps destabilize the overall steady state in which the effects of Processes A, B and C are balanced. Processes A and B separate so cleanly because Process A is an entirely non-radical process while Process B involves radicals. The detailed chemistry of Processes A, B and C in the presence of $CH_2(COOH)_2$ is given below. The non-intuitive numbering is the result of a historical artifact (Field et al. (1972)) in which reactions (R1) - (R5) are numbered according to the number of oxygen atoms in the transition state.

Process A is a series of non-radical reactions occurring at higher [Br^-] that remove Br^- and BrO_3^- with the simultaneous bromination of $CH_2(COOH)_2$ to yield $BrCH(COOH)_2$. Ce(IIII) is not oxidized to Ce(IV) during Process A because of the absence of radical, single-electron oxidants, e.g., $BrO_2^{\bullet}$.

$$Br^- + BrO_3^- + 2H^+ \rightleftharpoons HBrO_2 + HOBr \quad \text{(R3)}$$

$$Br^- + HBrO_2 + H^+ \rightarrow 2HBrO_2 \quad \text{(R4)}$$

$$3x(Br^- + HOBr + H^+ \rightleftharpoons Br_2 + H_2O) \quad \text{(R1)}$$

NET: $5Br^- + BrO_3^- + 6H^+ \rightarrow 3Br_2 + 3H_2O$

ADDING: $3Br_2 + BrO_3 + 3H^+ + 3CH_2(COOH)_2 \rightarrow 3BrCH(COOH)_2 + 3H_2O$

NET PROCESS A:

$$2Br^- + BrO_3^- + 3H^+ + 3CH_2(COOH)_2 \rightarrow 3BrCH(COOH)_2 + 3H_2O \quad \text{(A)}$$

Process B is a series of radical reactions occurring at lower $[Br^-]$ and relatively lower [Ce(IV)]/[Ce(III)] leading to the oxidation of Ce(III) to Ce(IV) and the auto-catalytic production of $HBrO_2$.

$$HBrO_2 + BrO_3^- + H^+ \rightleftharpoons Br_2O_4 + H_2O \rightleftharpoons 2BrO_2^{\bullet} + H_2O \quad \text{(R5)}$$

$$2x(BrO_2^{\bullet} + Ce(III) + H^+ \rightleftharpoons Ce(IV) + HBrO_2) \quad \text{(R6)}$$

NET:

$$HBrO_2 + BrO_3^- + 3H^+ + 2Ce(III) \rightleftharpoons 2HBrO_2 + 2Ce(IV) + H_2O \quad \text{(D)}$$

Finally,

$$2x(HBrO_2 + BrO_3^- + 3H^+ + 2Ce(III) \rightleftharpoons 2HBrO_2 + 2Ce(IV) + H_2O)$$

ADDING:

$$HBrO_2 + HBrO_2 \rightarrow HOBr + BrO_3^- + H^+ \quad \text{(R4)}$$

Overall Net:

$$4Ce(III) + BrO_3^- + 5H^+ \rightleftharpoons 4Ce(IV) + HOBr + 2H_2O \quad \text{(B)}$$

Note that Stoichiometry D is kinetically autocatalytic in $[HBrO_2]$. Stoichiometries A and B are in agreement with experiment. R.C. Thompson (Thompson (1971)) experimentally investigated the kinetics of stoichiometry B with Ce(III), Np(V), and Mn(II) and found the rate expression below, Eq 1, for $[Ce(III)] >> [BrO_3^-]$.

$$d[BrO_3^-]/dt = k_{experimental}[BrO_3^-]^2[H^+]^2 \quad (1)$$

The reaction rate of Process B is independent of both the concentration and the identity of the metal-ion! Application of the steady-state approximation to $[BrO_2^{\bullet}]$ and $[HBrO_2]$ (ignore Br_2O_4) in the mechanism of Process B with the assumption $k_6[Ce(III)][BrO_2^{\bullet}] >> k_{-5}[BrO_2^{\bullet}]^2$ yields Eq 2 (Noyes et al. (1971)).

$$d[BrO_3^-]/dt = (k_5^2/4k_4)[BrO_3^-]^2[H^+]^2 \quad (2)$$

Eq 2 suggests $k_{experimental} = ({k_5}^2 / 4k_4)$. The $[Br^-]_{crit}$ at which control passes be-

tween Process A and Process B resulting from the above mechanism can be calculated to be Eq 3.

$$[\mathrm{Br}^-]_{crit}=(k_5/k_2)[\mathrm{BrO}_3^-] \tag{3}$$

The values of all rate constants in Process A and B are reasonably well established (Field and Foersterling (1986); Hegedus et al. (2001)) and reproduce the experimental values of $k_{experimental}$ and $[\mathrm{Br}^-]_{crit}$.

Process C. The major overall effects of Process C are the reduction of Ce(IV) to Ce(III), the generation of $\mathrm{BrCH(COOH)_2}$, and the regeneration of Br^-. It is the necessity for accumulation of $\mathrm{BrCH(COOH)_2}$ that leads to the induction period before the onset of FKN oscillations. Process C is not as well understood as are Processes A and B. The net stoichiometry of the complete reaction of Ce(IV) with $\mathrm{CH_2(COOH)_2}$ is expected to be Eq 4.

$$\mathrm{CH_2(COOH)_2+6Ce(IV)+2H_2O\rightarrow 6Ce(III)+HCOOH+2CO_2+6H^+} \tag{4}$$

Remember that $\mathrm{BrCH(COOH)_2}$ is a product of the reaction of $\mathrm{Br_2}$ or HOBr with $\mathrm{CH_2(COOH)_2}$ in both Processes A and B. The net Stoichiometry of the complete reaction of Ce(IV) with $\mathrm{BrCH(COOH)_2}$ is given by Eq 5.

$$\mathrm{4Ce(IV)+BrCH(COOH)_2+2H_2O\rightarrow Br^-+4Ce(III)+HCOOH+2CO_2+5H^+} \tag{5}$$

Process C is the sum of Stoichiometries (4) and (5) and is the origin of the Br^- that poisons Process B by reaction R2 when the rate of Process C is sufficiently high. However Stochiometries (4) and (5) are not well understood. Process C typically does not go to completion with substantial amounts of $Br_2C(COOH)_2$ and Br_3COOH accumulating during the BZ reaction. There are many potential partially oxidized intermediate organic species such as $HOCH(COOH)_2$, $O{=}C(COOH)_2$, HOCH(COOH), and decarboxlated species such as $HOCH_2(COOH)$ that may accumulate. Not all potential partially oxidized organic derivatives of $CH_2(COOH)_2$ have been detected in BZ mixtures. There also are many organic radical species potentially present, e.g., $^{\cdot}CH(COOH)_2$, $CH_2(COOH)(COO^{\cdot})$, $BrO_2^{\cdot}$, and $^{\cdot}OCH(COOH)_2$. Radical species seem to largely disappear via radical-combination processes (Hegedus et al. (2001)).

The important feature of Process C is that it generates Br^- from a mixture of Ce(IV), $CH_2(COOH)_2$, HOBr, and $BrCH(COOH)_2$. The stoichiometry of Br^- production per Ce(IV) in Process C is most important to the appearance of oscillation in the full system, as will be seen in the next section. Most FKN mechanisms of Process C do not produce sufficient Br^- for oscillations to occur, suggesting that there are reactions of $BrCH(COOH)_2$ (or other bromine-containing species) with species other than Ce(IV) (perhaps radical intermediates) that lead to Br^-.

1.3.2 Uncatalyzed Belousov-Zhabotinsky Oscillators

Oscillations in redox potential were observed by Babu and Srinivasulu (Babu and Srinivasulu (1976)) during oxidation of Gallic Acid (3,4,5 - benzoic acid) by BrO_3^- in the presence of Co ion. These oscillations were unexpected because even in a strongly acid medium BrO_3^- does not have the potential to oxidize uncomplexed Co(II) to Co(III). This was noted by Körös and Orbán (Orban and Koros (1978b)), who thus found Br^--controlled FKN-like oscillations in redox potential even in the absence of Co ion. Kuhnert and Linde (Kuhnert and Linde (1977)) had reported an uncatalyzed oscillator a year earlier using *p*-diethylaminobenzenediazonium tetrafluoroborate as organic substrate. Orbán and Körös (Orban and Koros (1978a)) list 23 phenol and aniline derivatives that may serve as organic substrate in uncatalyzed BrO_3^- oscillators.

Essentially all metal-ion catalyzed BZ oscillators form CO_2 bubbles that disrupt pattern formation. However, Farage and Janjic (Farage and Janjic (1982b,a)) reported uncatalyzed oscillation in a the BrO_3^--cyclohexanedione (CHD) oscillator present in the anomalous dispersion system discussed above. An significant advantage of this system is that the cyclohexane ring in CHD is not broken during the reaction but is instead converted to quinones without the release of CO_2. The mechanism of the CHD-BrO_3^--$Fe(phen)_3^{3+}/Fe(phen)_3^{2+}$ system has been considered carefully by Szalai et al. (Szalai et al. (2003)) and is discussed below.

The mechanistic details of the uncatalyzed BrO_3^--CHD (Britton (2003); Koros et al. (1998)) and the metal-ion (typically $Fe(phen)_3^{3+}/Fe(phen)_3^{2+}$)-catalyzed BrO_3^--CHD (Szalai et al. (2002, 2003)) systems have been studied in some detail.

It seems clear that the active organic species are in fact derivatives of the starting organic substrate, CHD. The organic chemistry suggested by the above authors is shown in Figure 4.

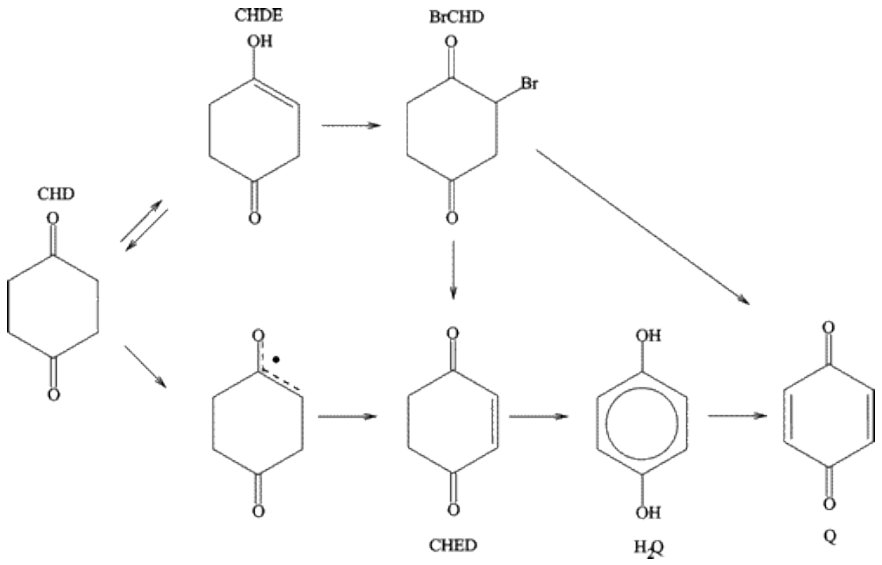

Figure 4: Key Organic Species in the Oxidation of 1,4-cyclohexanedione by Bromate (Upper Pathway) and by Catalyst (Lower Pathway).
Abbreviations: CHD, 1,4-cyclohexanedione; CHDE, enol form of CHD; BrCHD, 2-bromo-1,4-cyclohxanedione; CHED, 2-cyclohexane-1,4-dione; H_2Q, 1,4-hydroquinone; Q, 1,4-benzoquinone. From I. Szalai, K. Kurin-Csörgei, I. R. Epstein, and M. Orbán, *J. Phys. Chem. A*, **2003**, *107*, 10074-10081.

The experimentally identified intermediate 1,4-hydroquinone (H_2Q) is thought to be produced at a constant rate from BrCHD and eventually oxidized autocatalytically to 1,4-benzoquinone (Q). It seems to be the time-scale separation between the slow accumulation and the autocatalytic consumption of H_2Q that leads to oscillatory behavior. This suggests that the uncatalyzed mechanism is more related to an empty-refilling dynamics (Tinsley and Field (2001)) than to the switching (relaxation) FKN mechanism.

The actual chemical mechanism used in simulations by Szalai et al. (Szalai et al.

(2003)) comprises Processes A and B from the FKN mechanism, the reactions below (S1 - S3) involving the oxidized form (Ox^{n+}) and reduced form ($Red^{(n-1)+}$) of the metal-ion catalyst, as well as reactions coupling the various reaction sets.

$$2Ox^{n+} + CHD \rightarrow 2Red^{(n-1)+} + H_2Q + 2H^+ \quad \text{(S1)}$$

$$2Ox^{n+} + BrCHD \rightarrow Q + Br^- + 2Red^{(n-1)+} \quad \text{(S2)}$$

$$2Ox^{n+} + H_2Q \rightarrow 2Red^{(n-1)+} + Q + 2H^+ \quad \text{(S3)}$$

Szalai et al. (Szalai et al. (2003)) developed a model that comprised 30 reactions and 16 variables (chemical species). Most rate constants in this system have been determined previously (Szalai et al. (2002)). Simulations based on this model reproduce well the observed well-stirred temporal behavior of BrO_3^--CHD-metal-ion systems

1.4 Skeleton Models of Oscillatory Chemistry

Theoretical work on oscillations resulting from nonlinear dynamic equations largely has been based on simple models with dynamics expressed as polynomial differential equations.

1.4.1 The Lotka-Volterra Model

This model is largely due to Alfred Lotka (Lotka (1910)) who showed that a set of two consecutive chemical reactions can give rise to damped oscillation when occurring far from chemical equilibrium. He continued his work on oscillating chemical reactions

resulting from mass action kinetics in a later paper (Lotka (1920)). These models are not related to any known chemical reaction, but have been of considerable interest to ecologists and were noted by W.C. Bray (Bray (1921)) in his early investigation of the IO_3^--catalyzed decomposition of H_2O_2. The best-known model resulting from Lotka's early work is referred to as the Lotka-Voltera model (Nicolis and Prigogine (1977)) and is typically applied to predator-prey dynamics.

The Lotka-Volterra model is presented as a set of three, coupled, simple, irreversible transformations (perhaps chemical) whose dynamics is governed by mass-action kinetics. It contains two variable species, X and Y and four parameters, k_{LV1}, k_{LV2}, k_{LV3}, and A.

$$\mathrm{A}+\mathrm{X} \rightarrow 2\mathrm{X} \tag{LV1}$$

$$\mathrm{X}+\mathrm{Y} \rightarrow 2\mathrm{Y} \tag{LV2}$$

$$\mathrm{Y} \rightarrow \mathrm{P} \tag{LV3}$$

$$\mathrm{A} \rightarrow \mathrm{P}$$

A set of differential equations can be generated to describe the behavior of predator (y = bobcats) and prey (x = rabbits) species on the basis of transformations LV1 - LV3.

$$dx/dt = k_{LV1}\mathrm{a}x\text{-}k_{LV2}xy \tag{5}$$

$$dy/dt = k_{LV2}xy\text{-}k_{LV3}y \tag{6}$$

Reaction LV1 is the autocatalytic (+ $k_{LV1}ax$) growth of rabbits from grass (A) in dx/dt. Reaction LV2 is the autocatalytic growth of bobcats (+ $k_{LV2}xy$ in dy/dt) with loss of rabbits (- $k_{LV2}xy$ in dx/dt). Reaction LV3 is the loss of bobcats (- $k_{LV3}y$ in dy/dt). Autocatalysis typically appears in oscillatory, mass-action models. In the case of simple autocatalysis as in the Lotka-Volterra model, there must be two autocatalytic steps to destabilize the $dx/dt = dy/dt = 0$ steady state.

The Lotka-Volterra model otherwise is not a very good model of a chemical system (Epstein and Pojman (1998); Epstein et al. (2006)). It oscillates at a unique period and amplitude for any particular set of values of k_{LV1}, k_{LV2}, k_{LV3}, A, and initial values of x and y. The model responds to perturbation of x and y by moving to a new orbit. Real oscillatory chemical systems do not behave in this manner. They instead approach an oscillatory orbit referred to as a limit cycle (Epstein and Pojman (1998); Strogatz (2001)) whose period and amplitude is determined by the values of the parameters of the system, i.e., k_{LV1}, k_{LV2}, k_{LV3}, and A. This limit cycle is furthermore asymptotically approached, when the steady state is unstable, by trajectories starting from any physically realistic initial condition.

1.4.2 The Brusellator Model

The simplest model based on mass-action kinetics and exhibiting limit-cycle oscillations was proposed by Prigogine and Lefevre (Lefever et al. (1967)) and dubbed the "Brusselator" by Tyson (Tyson (1973)). Its origin seems to be related to a more

complex model proposed by Turing (Turing (1952)) as "The Chemical Basis of Morphogenesis". The Brusselator is closely related to no real chemical reaction. However, it is rich dynamically and its investigation has been instructive (Nicolis et al. (1975); Nicolis and Prigogine (1977, 1989)). Its major importance lies in its demonstration that a mechanism of chemical form can show homogeneous oscillation and traveling waves such as seen experimentally in the BZ system.

The Chemical form of the Brusselator is given below (B1 - B4).

$$\mathrm{A} \rightleftharpoons \mathrm{X} \tag{B1}$$

$$2\mathrm{X}+\mathrm{Y} \rightleftharpoons 3\mathrm{X} \tag{B2}$$

$$\mathrm{B}+\mathrm{X} \rightleftharpoons \mathrm{Y}+\mathrm{D} \tag{B3}$$

$$\mathrm{X} \rightleftharpoons \mathrm{E} \tag{B4}$$

$$\mathrm{A}+\mathrm{B} \rightleftharpoons \mathrm{C}+\mathrm{D}$$

Exploration of the near-to-equilibrium behavior of the Brusselator is normally done with the reverse rate constants set to one. The far-from-equilibrium dynamic behavior of the Brusselator is investigated with the reverse rate constants set to zero. The mass-action kinetics for this irreversible case are given below.

$$dx/dt = k_1 A + k_3 x^2 y - k_3 B x - k_4 x \tag{7}$$

$$dy/dt = - k_2x^2y + k_3Bx \quad (8)$$

The Brusselator shows a variety of limit-cycle and spatial-pattern behaviors. Tyson and Light (Tyson and Light (1973)) showed that the trimolecular step (B2) is necessary for the appearance of limit cycle oscillations in a two-variable, polynomial system.

1.4.3 The Oregonator Reduced Model of the FKN Mechanism

The FKN mechanism described above for the BrO_3^-- Ce(IV)/Ce(III) - $CH_2(COOH)_2$ - H_2SO_4 oscillator may be reduced to a variety of simple models (Gyorgyi and Field (1991)) similar to the Lotka-Volterra or Brusselator models except that these models are closely related to a real oscillating chemical reaction. The simplest of these models is referred to as the Oregonator (Field and Noyes (1974a)) because of its origin at the University of Oregon.

The major Oregonator variables are $X \equiv HBrO_2$; $Y \equiv Br^-$; $Z \equiv 2Ce(IV)$; $P \equiv$ HOBr or $BrCH(COOH)_2$, and $A \equiv BrO_3^-$. The reduction process leading to the simple Oregonator is described below.

Reaction (R3), $BrO_3^- + Br^- + 2H^+ \rightleftharpoons HBrO_2 + HOBr$, becomes (O3) in the Oregonator, A+Y$\rightleftharpoons$X+P, with $k_{O3} = k_{R3}\,[H^+]^2$, $k_{R3} = 2\ M^{-3}s^{-1}$ and $k_{-O3} = k_{-R3} = 3.2\ M^{-1}s^{-1}$. Reaction (R3) is often substantially reversible during the BZ oscillations, but this reversibility is typically neglected in the simple Oregonator. Reaction (R2), $HBrO_2 + Br^- + H^+ \rightarrow 2HOBr$ becomes (O2), X+Y$\rightarrow$2P, with $k_{O2} = k_{R2}\,[H^+]$ and $k_{R2} = 3x10^6\ M^{-1}s^{-1}$. Reaction (R1) followed by the bromination of $CH_2(COOH)_2$ is assumed to be the ultimate fate of nearly all HOBr and Br_2. Thus we ignore these

reactions and instead consider the species P to be $BrCH(COOH)_2$ rather than HOBr.

Process B It is assumed in simplification of Process B that nearly all $BrO_2^{\cdot}$ produced in reaction (R5) reacts rapidly with Ce(III) in reaction (R6). This implies reaction (R5) is not reversible, making it rate-determining for reaction (R6). If reaction (R6) is also assumed not to be reversible, reaction (R5) becomes rate-determining for Stoichiometry (D) as well. Thus for each $HBrO_2$ that disappears via reaction (R5), two Ce(IV) ions and two $HBrO_2$ molecules are generated. For the above approximations to be correct it must be so that Rate (R6) = k_{R6} [Ce(III)][$BrO_2^{\cdot}$][H^+] >> Rate (-R5) = $2k_{-R5}$ [$BrO_2{\cdot}$]^2 or k_{R6} [Ce(III)][H^+] >> k_{-R5} [$BrO_2{\cdot}$]. Using well-known values of k_{-R5} and k_{R6} (Field et al. (1972); Field and Foersterling (1986); Hegedus et al. (2001)) and reasonable estimates of [Ce(III)] and [$BrO_2{\cdot}$] when Process B is dominant during the BZ oscillations, we find (6.2x10^6 M^{-2} s^{-1})(0.0005 M)(0.8 M) = 2480 s^{-1} >> (2x10^7 $M^{-1}s^{-1}$)(1x10^{-6} M) = 20 s^{-1}. Thus the assumption that reaction (R5) is rate determining for reaction (R6) in the forward direction is supported, and we define the third-step of the Oregonator (reaction O5) as analogous to Stoichiometry (D)

$$A + X \rightarrow 2X + Z \qquad \text{(O5)}$$

Recall that Z $\equiv$ 2 Ce(IV). The rate constant $k_{O5} = k_{R5}$ [BrO_3^-][H^+] with k_{R5} = 42 $M^{-2}s^{-1}$. Note that the parameter A (BrO_3^-) is absorbed into $k_{O5.}$

It turns out that reaction (R6) is significantly reversible. This complication is usually ignored in order to preserve the simple form of reaction (O5). However, the reversibility of reaction (R5) may be readily accounted for by adding the multiplica-

tive term (C_0 - Z/2)/C_0 to k_{O5} in order to diminish the rate of reaction (O5) as Z accumulates. Thus we have $k_{O5} = k_{R5}$ {(C_0 - Z/2)/C_0} [BrO_3^-][H^+] when the reversibility of (O5) needs to be considered. The quantity C_0 is the total of the oxidized and reduced forms of the metal-ion catalyst, e.g., C_0 = [Ce(III)] + [Ce(IV)].

Reaction (R4) is readily converted to reaction (O4) by simple identity to yield

$$\mathrm{X+X \rightarrow A+P} \qquad k_{O4}=k_{R4}=3\mathrm{x}10^3 M^{-1}s^{-1} \qquad \text{(O4)}$$

Process C reduces Ce(IV) back to Ce(III) with the regeneration of Br^- during dominance of the system by Process B. This increase in [Br^-] and decrease in [Ce(IV)]/[Ce(III)] eventually resets the BZ cycle to Process A. It is this negative feedback coupled with the autocatalytic nature of Process B that destabilizes the BZ steady state in favor of limit cycle oscillation. Process C can be imagined as the combination of reactions (4) and (5) together reducing Ce(IV) and generating Br^-.

$$\mathrm{CH_2(COOH)_2+6Ce(IV)+2H_2O \rightarrow 6Ce(III)+HCOOH+2CO_2+6H^+} \qquad (4)$$

$$\mathrm{4Ce(IV)+BrCH(COOH)_2+2H_2O \rightarrow Br^-+4Ce(III)+HCOOH+2CO_2+5H^+} \qquad (5)$$

However there are stoichiometric problems. If reactions (4) and (5) both occur as written, then for each ten Ce(IV) reduced only one Br^- is released. This is not enough Br^- to disable the autocatalysis in Process B by winning the competition between reactions (R2) and (R5) for $HBrO_2$. Indeed linear stability analysis (Field and Noyes (1974a); Epstein and Pojman (1998); Freire et al. (2009)) of the Oregonator shows

that a minimum of one Br^- must be generated for each Ce(IV) reduced for the FKN steady state to be destabilized and the system evolve to limit-cycle oscillation.

It seems apparent that for sufficient Br^- to be produced by reactions (4) and (5) to destabilize the steady state then $CH_2(COOH)_2$ and $BrCH(COOH)_2$ are likely not reduced all the way to the stoichiometric final products of HCOOH and CO_2. Potential products not oxidized by Ce(IV) might include $HOCH(COOH)_2$ and $O{=}C(COOH)_2$. It also seems likely that organic radical species such as $^{\cdot}CH(COOH)_2$, $^{\cdot}OCH(COOH)_2$ or $^{\cdot}CH_2COOH$ might bite on $BrCH(COOH)_2$ to yield excess Br^-, although the major fate of radicals in Process C seems to be dimerization (Hegedus et al. (2001)). Thus Process C is not well understood mechanistically and Process C is represented in the Oregonator by the generic reaction (OC).

$$B{+}Z \rightarrow {}^1\!/_2 fY \qquad k_{OC}{=}1 \qquad \text{(OC)}$$

The quantity B is typically taken to be $[CH_2(COOH)_2]_0$. The quantity f is the stoichiometric factor defining how many Br^- are produced per Ce(IV) reduced. The two factor results because Z = 2 Ce(IV).

Thus the Oregonator model becomes Reactions O2 - OC.

Process A

$$A{+}Y \rightarrow X{+}P \qquad k_{O3}{=}k_{R3}[H^+]^2 \qquad \text{(O3)}$$

$$X{+}Y \rightarrow 2P \qquad k_{O2}{=}k_{R2}[H^+] \qquad \text{(O2)}$$

Process B

$$\text{A+X}\rightarrow\text{2X+Z} \qquad k_{O5}=k_5\{(C_0\text{-Z}/2)/C_0\}[\text{BrO}_3^-][\text{H}^+] \qquad \text{(O5)}$$

$$\text{X+X}\rightarrow\text{A+P} \qquad k_{O4}=k_{R4} \qquad \text{(O4)}$$

Process C

$$\text{B+Z} \rightarrow {}^1\!/_2\text{fY} \qquad \text{k}_{OC}=\text{expendable} \qquad \text{(OC)}$$

The Oregonator dynamic equation for a well-stirred batch reactor is shown below.

$$\frac{d\text{X}}{dt} = k_3AY\text{-}k_2XY\text{+}k_5AX\text{-}2k_4X^2 \qquad (9)$$

$$\frac{d\text{Y}}{d\text{t}} = k_3AY\text{-}k_2XY\text{+}{}^1\!/_2\text{f}\ \ k_cBZ \qquad (10)$$

$$\frac{d\text{Z}}{d\text{t}} = 2k_5AX\text{-}k_cBZ \qquad (11)$$

Equations (6) - (8) may be investigated by analytical methods and by numerical integration, as is done here.

Equations (9) - (11) may be expressed in dimensionless form as below.

$$\frac{dx}{d\tau} = \{(qy\text{-}xy\text{+}x(1\text{-}x)\}/\varepsilon \qquad (12)$$

$$\frac{dy}{d\tau} = (\text{-}qy\text{-}xy\text{+}fz)/\varepsilon' \qquad (13)$$

$$\frac{dz}{\text{d}\tau} = x\text{-}z \qquad (14)$$

with variable scalings $x = 2k_4X/k_5A$; $y = k_2Y/k_5A$; $z = k_ck_4\ BZ/(k_5A)^2$; $\tau = k_CBt$ and parameter scalings $\varepsilon = k_CB/k_5A$; $\varepsilon' = 2k_Ck_4B/k_2k_5A$; and $q = 2k_3k_4/k_2k_5$. Typical parameter values for $A = 0.06$ M and $B = 0.02$ M are $\varepsilon = 1\text{x}10^{-2}$, $\varepsilon' = 2.5\text{x}10^{-5}$; $q = 9\text{x}10^{-5}$.

The advantages of scaling a set of differential equations include (1) they may assume a simpler form, e.g., compare Eqs (9) - (11) and Eqs (12) - (14), and (2) small parameters may appear in the scaled equations that may allow a system of equations to be reduced by changing a differential equation to an algebraic equation. Furthermore, nullcline methods (Gray and Scott (1990)) of investigation of sets of differential equations are often simplified by scaling the equations (Scott (1994)).

As an example (Scott (1994)) of reducing a set of scaled differential equations may be seen by inspecting Eqs (12) - (14). Rearrangement of Eq (13) yields

$$(\varepsilon')dy/d\tau = -qy - xy + fz \tag{15}$$

Recall $\varepsilon' = 2.5\text{x}10^{-5}$. On the crudest approximation we then assume $\varepsilon' = (dy/d\tau) = 0$. Thus equation (12) becomes $0 = (-\ qy\ -\ xy\ +\ fz)$ or $y = y_{steadystate} = fz/(q + x)$. Substituting this result into Eqs. (9) and (11) yields a reduced set of two equations, Eqs. (16) and (17).

$$\varepsilon\left(\frac{dx}{d\tau}\right) = x(1-x) - \{(x-q)/(q+x)\}fz \tag{16}$$

$$\frac{dz}{d\tau} = x - z \tag{17}$$

Methods of differential equation reduction are much more subtle and powerful than shown in this simple example (Kalachev and Field (2001)).

2 The Anomalous Wave Dispersion Model

The model used here for simulation of anomalous wave-dispersion in the CHD-BZ reaction consists of six dynamic variables, representing the most important chemical species, and two parameters, representing the concentrations of the major pool reactants bromate and and cyclohexanedione. The model is of polynomial form and is constructed by mass-action. We begin with an analysis of the model in a well-stirred batch system, which exhibits only spatially homogeneous temporal dynamics. The analysis then continues to spatially distributed systems including the interaction of reaction and diffusion and the development of traveling spatial waves where the phenomenon of anomalous wave dispersion may appear.

2.1 The Mass-Action Equations

$$\begin{aligned}
\mathrm{X+Y} &\rightarrow \mathrm{P} && (1)\\
\mathrm{A+Y} &\rightarrow \mathrm{X} && (2)\\
\mathrm{X+X} &\rightarrow \mathrm{A} && (3)\\
\mathrm{A+X} &\rightarrow \mathrm{2X+2Z+gJ} && (4)\\
\mathrm{Z+B} &\rightarrow \frac{1}{2}\mathrm{fY} && (5)\\
\mathrm{J+M} &\rightarrow \mathrm{2M} && (6)\\
\mathrm{M+Y} &\rightleftharpoons \mathrm{Q} && (7)\\
\mathrm{M+M} &\rightarrow && (8)
\end{aligned}$$

The variables f and g are stoichiometric factors, and are treated as expendable parameters. Species included in the mechanism are X≡$HBrO_2$, Y≡Br^-, Z≡$[Fe(phen)_3]^{3+}$

k_1	4.0x10^7 $M^{-2}s^{-1}$
k_2	2.0 $M^{-3}s^{-1}$
k_3	9.0x10^3 $M^{-2}s^{-1}$
k_4	42.0 $M^{-2}s^{-1}$
k_5	0.5 $M^{-1}s^{-1}$
k_6	70.0 $M^{-1}s^{-1}$
k_{7f}	5.0x10^4 $M^{-1}s^{-1}$
k_{7r}	5.0x10^{-4} s^{-1}
k_8	35.0 $M^{-1}s^{-1}$

Table 1: Rate Constants

(phen≡1,10-Phenanthroline). The identities of the remaining species are not specifically defined but can be speculated upon. The species J is most likely a brominated or oxidized organic byproduct of the auto-catalytic production of bromous acid. The species M is similar, while species Q is a brominated organic. These identifications will be discussed further.

The first five reactions constitute the oscillatory Oregonator mechanism (Field and Noyes (1974a)), which is a well understood model of the Belousov-Zhabotinsky reaction. Reactions 6-8 are a second pathway for the oxidation of organic substrate, coupled to the Oregonator to provide non-monotonic recovery of Br^- to the steady state after an autocatalytics pulse of oxidation (Process B). The model can be considered a heuristic skeleton model to provide dynamics favorable to reproducing anomalous dispersion in a wave train simulation.

The model can be written as a series of differential equations.

$$
\begin{aligned}
R1 &= k_1 XYH \\
R2 &= k_2 AYH^2 \\
R3 &= k_3 X^2 H \\
R4 &= k_4 AHX(1 - Z/C_0) \\
R5 &= k_5 BZ \\
R6 &= k_6 JM \\
R7_f &= k_{7f} YM \\
R7_r &= k_{7r} Q \\
R8 &= k_8 MM
\end{aligned}
\tag{9}
$$

$$
\begin{aligned}
\tfrac{dX}{dt} &= -R1 + R2 - 2.0R3 + R4 \\
\tfrac{dY}{dt} &= -R1 - R2 + \tfrac{1}{2} fR5 - R7_f + R7_r \\
\tfrac{dZ}{dt} &= 2.0R4 - R5 \\
\tfrac{dJ}{dt} &= gR4 - R6 \\
\tfrac{dM}{dt} &= R6 - R7_f + R7_r - 2.0R8 \\
\tfrac{dQ}{dt} &= R7_f - R7_r
\end{aligned}
\tag{10}
$$

It is important to note the mass-balance term, $(1 - Z/C_0)$, present in $R4$. The inclusion of the ratio of ferroin to that of the total catalyst concentration limits uncontrolled growth of the ferriin concentration. This is necessary to account for the reversability of Process B over a wide range of reaction conditions. C_0=3.0x10^{-3} in all calculations, unless explicitly stated otherwise.

2.2 Chemical Processes

2.2.1 The Oregonator

The Oregonator as described previously consists of the following equations

Process A

$$\text{A+Y} \rightarrow \text{X+P} \qquad k_{O3} = k_{R3}[\text{H}^+]^2 \qquad \text{(O3)}$$

$$\text{X+Y} \rightarrow \text{2P} \qquad k_{O2} = k_{R2}[\text{H}^+] \qquad \text{(O2)}$$

Process B

$$\text{A+X} \rightarrow \text{2X+Z} \qquad k_{O5} = \{(C_0\text{-Z}/2)/C_0\}[\text{BrO}_3^-][\text{H}^+] \qquad \text{(O5)}$$

$$\text{X+X} \rightarrow \text{A+P} \qquad k_{O4} = k_{R4} \qquad \text{(O4)}$$

Process C

Process C refers to the regeneration of Br^- via the products of Process B. The classic FKN understanding of Process C suggests that the organic substrate can be brominated through HOBr, probably via the formation of Br_2. In the CHD-BZ system cyclohexanedione and the brominated species react with ferriin catalyst, oxidizing the organic species, and resulting in bromide ion and reduced catalyst.

$$2\text{Z}_{ox}\text{+CHD+BrCHD} \rightarrow f\text{Br}^-\text{+2Z}_{red}\text{+other products} \qquad \text{(OC)}$$

The stoichiometric factor, f, used in the reaction is an adjustable parameter that describes the amount of Br^- produced during the process. If the reaction proceeds exclusively via brominated organic species, f=2. In the analysis we have taken f is a constant, although it has been used as a dynamic variable in other studies (Janz et al. (1980)). It is also worth noting that stoichiometric factors with a value greater than two seem to violate the stoichiometry of the reaction. With respect to the FKN mechanism this concern has been addressed through a chain-mechanism involving malonyl radicals and bromine atom radicals (Gyorgyi et al. (1990)).

2.2.2 The Modified Oregonator

To create a model that exhibits the phenomenon of anomalous wave-dispersion an extension to the Oregonator has been constructed. This consists of three new reactions and an additional product in Process B, which then becomes

$$BrO_3^- + HBrO_2 + 2Z_{red} + 3H^+ \rightarrow 2HBrO_2 + 2Z_{ox} + H_2O + gJ$$

where g is an expendable stoichiometric coefficient and J is a byproduct of Process B. The three additional reactions are as follows:

$$J + M \rightarrow 2M \tag{6}$$

$$M + Y \rightleftharpoons Q \tag{7}$$

$$M + M \rightarrow \tag{8}$$

In this model Process C consists of Reactions 5-8. Several conjectures can be made concerning the identity of the unnamed species, J, M and Q, in the modified Oregonator reactions. In the absence of experimental observations, the mechanism must be judged predominantly in terms of what it accomplishes. The added reactions provide a second, uncatalyzed, pathway for the oxidation of the organic substrate. The time scale for the uncatalyzed pathway is sufficiently different from the catalyzed Oregonator mechanism that new behavior of anomalous wave-dispersion can be observed.

The model equations were integrated using FORTRAN77 driver code and the Livermore Solver for Ordinary Differential Equations (LSODES) (Hindmarsh (1980)). All results were obtained using the six-variable modified Oregonator mechanism, unless otherwise specified.

2.3 Stability Analysis

The stability of the system is determined by the eigenvalues of the Jacobian matrix, evaluated at the steady state, defined by the six differential equations. By calculating the steady states of the system for any set of parameters, the Jacobean matrix can be evaluated, and the stability of the system determined. This allows us to determine for which values of the principal bifurcation parameters the system is stable, or oscillatory.

2.3.1 Linearized system

The evolution (growth or decay) of a small disturbance from the steady-state defines the stability of the system. By linearizing the system near to the steady-state it is possible to determine the stability of that fixed point.

For a two dimensional system,

$dx/dt = f(x, y)$

$dy/dt = g(x, y)$

let $f(x*, g*) = 0$, $g(x*, y*) = 0$

Which denotes x*,y* as a steady state. A small perturbation to the steady state can be defined as

$u = x - x*, v = y - y*$

Forming differential equations for u and v through a Taylor series expansion allows us to determine whether the perturbation grows, or returns to the steady state.

$\frac{du}{dt} = u\frac{\partial f}{\partial x} + v\frac{\partial f}{\partial y} + O(u^2, v^2, uv)$

$\frac{dv}{dt} = u\frac{\partial g}{dx} + v\frac{\partial g}{dy} + O(u^2, v^2, uv)$

Here $O(u^2,v^2,uv)$ is a shorthand representation of quadratic terms arising from the Taylor expansion. Since the values of u and v are very small, the quadratic terms can be eliminated, limiting the analysis to the linear regime very close to the steady

state. Writing the above in matrix notation gives us the following

$$\begin{bmatrix} \frac{du}{dt} \\ \\ \frac{dv}{dt} \end{bmatrix} = \begin{bmatrix} \frac{\partial f}{\partial x} & \frac{\partial f}{\partial y} \\ \\ \frac{\partial g}{\partial x} & \frac{\partial g}{\partial y} \end{bmatrix} \begin{bmatrix} u \\ \\ v \end{bmatrix} + \text{quadratic terms}$$

The matrix

$$\text{A}= \begin{bmatrix} \frac{\partial f}{\partial x} & \frac{\partial f}{\partial y} \\ \\ \frac{\partial g}{\partial x} & \frac{\partial g}{\partial y} \end{bmatrix}$$

evaluated at (x*,y*) is the Jacobian matrix for the system of differential equations. The eigenvalues of this matrix indicate the stability of the fixed point (x*,y*). If the real parts of the eigenvalues are negative, then a small perturbation will decay to the steady state. Conversely, if the real part of any eigenvalue is positive, the result of a small perturbation will result in motion away from the steady state. An analysis of the stability of the modified Oregonator was performed by solving for the steady-state and evaluating the resulting Jacobian matrix. For example, fig. 5 shows for what values of f the system is stable, with A=0.06, B=0.02, H=1.0, g=0.1. For clarity a dashed line is included at zero on the y-axis. For any value of f where the eigenvalue is positive, a stable limit cycle may exist. The plot shows that while varying f and holding all other parameters constant the system transitions from stability to instability at $f \approxeq 0.615$, and returns to stability at $f \approxeq 2.07$.

2.3.2 Analysis of Bifurcation Type

The points at which the eigenvalues pass through zero are Hopf bifurcations where a pair of eigenvalues of the Jacobian exist as complex conjugates. The change of sign (passage through zero) of the real part of the complex conjugate pair defines the point where stability changes. In the Oregonator model bifurcations may be either subcritical or supercritical; the low-f bifurcation is often subcritical while the high-f bifurcation is often supercritical. The figures 6 and 7 show the effect of a small perturbation to Y on this system at $f \approxeq 0.55$, in the neighborhood of the low-f

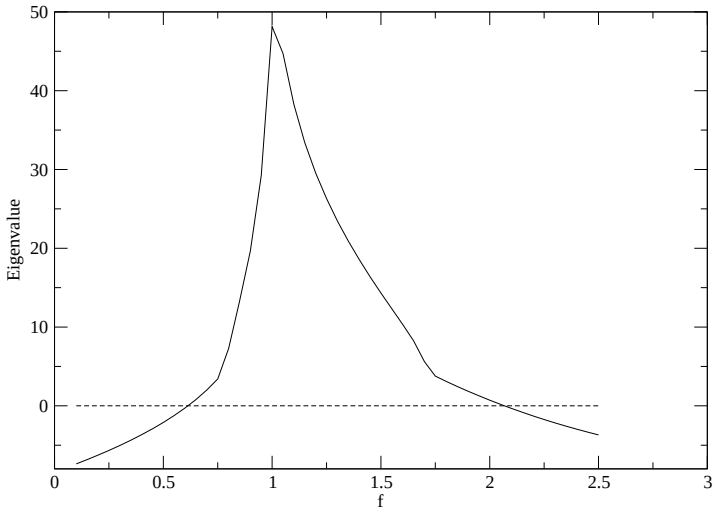

Figure 5: Bifurcation Diagram of Equations 1-8
A=0.06, B=0.02, H=1.0, g=0.1

bifurcation. Figure 6 shows that a small perturbation results in damped oscillations rapidly decaying to the steady state. Figure 7 is the result of a slightly larger perturbation, which moves the system to the surrounding stable limit cycle. This is an example of hysteresis occuring in the vicinity of a subcritical Hopf bifurcation where there is a coexistence of a steady state, an unstable limit cycle, and a stable limit cycle. As f increases the steady state remains stable until crossing the bifurcation point, and the system evolves to the already existing limit cycle. If f continues to increase to the second, supercritical, bifurcation oscillations decay to zero-amplitude as the steady-state regains stability.

2.3.3 Mapping Stability

Maps of stability can be created by evaluating the modified Oregonator over a variety of parameter values. These maps are useful in determining excitable conditions that are necessary for the formation of traveling chemical waves.

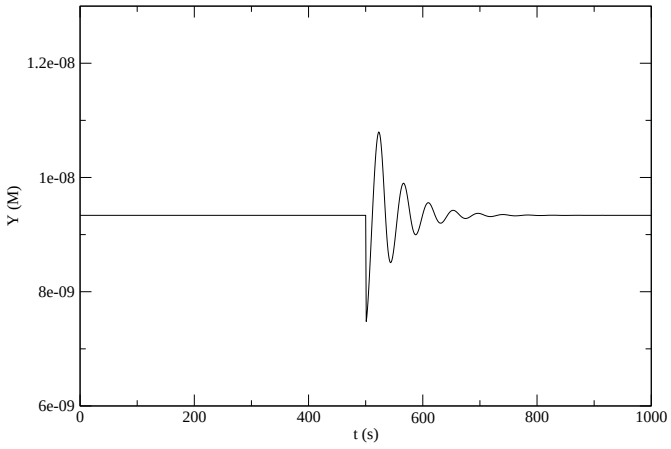

Figure 6: Sub-Critical Relaxation Resulting from a Perturbation of the Steady-state

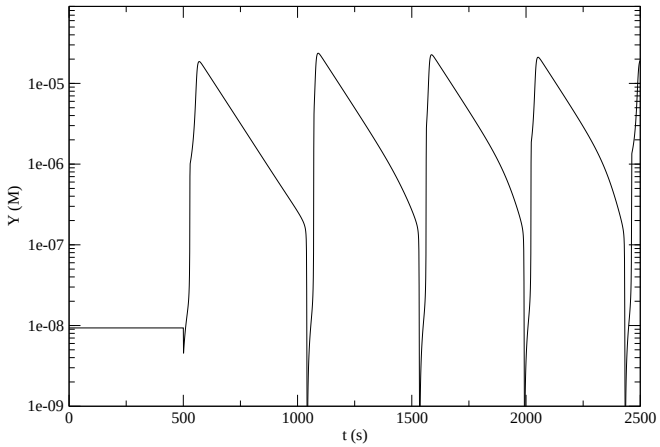

Figure 7: Large Perturbation Leading to Sub-critical Excitation to the Limit Cycle

Figure 8: Exploration of parameters f (abscissa) and H (ordinate) on regions of stability and instability at various values of parameters A and B

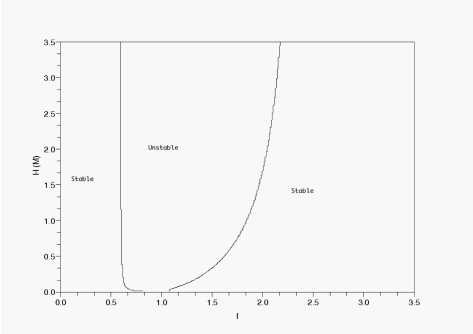

(a) A=0.06 M, B=0.02 M

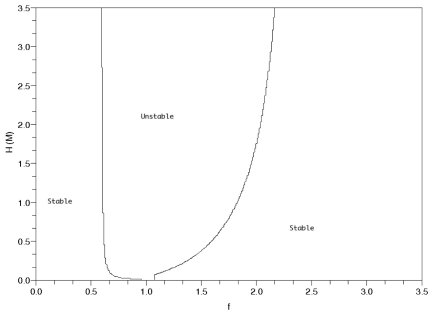

(b) A=0.06 M, B=0.02 M

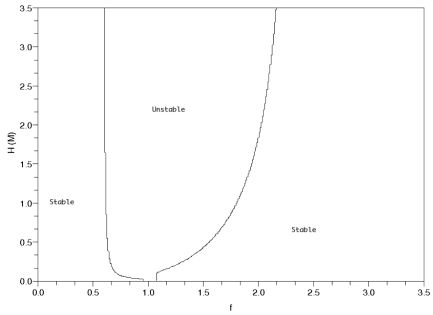

(c) A=0.06 M, B=0.1 M

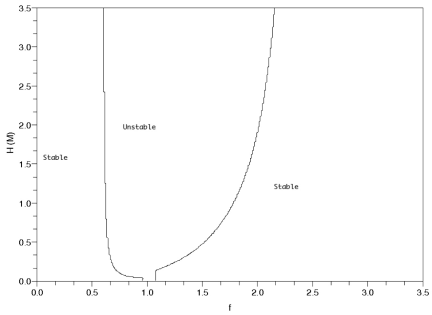

(d) A=0.06 M, B=0.15

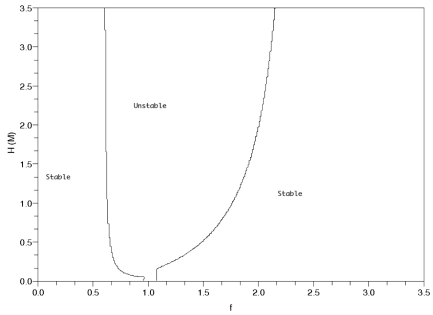

(e) A=0.06 M, B=0.2 M

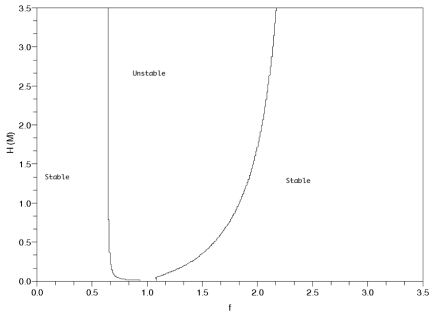

(f) A=0.1 M, B=0.5 M

Figure 9: Exploration of parameters f (abscissa) and H (ordinate) on regions of stability and instability at various values of parameters A and B

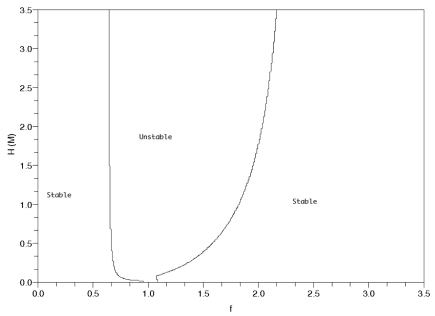

(a) A=0.1 M, B=0.1 M

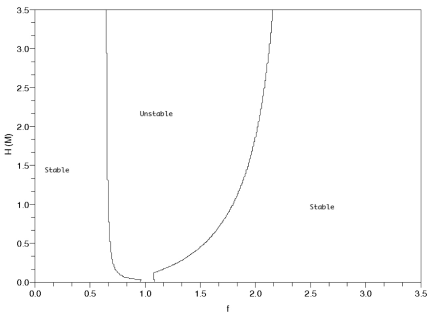

(b) A=0.1 M, B=0.2 M

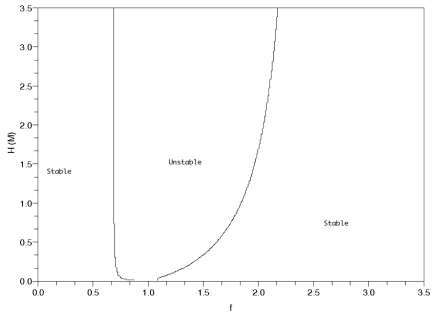

(c) A=0.15, B=0.05

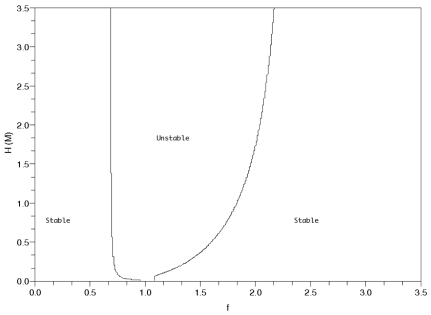

(d) A=0.15 M, B=0.1 M

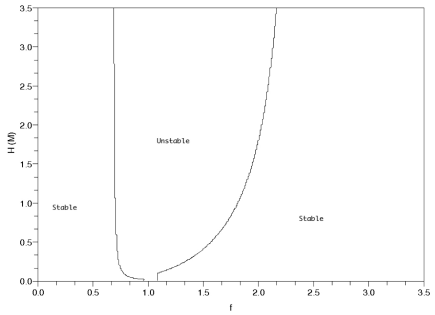

(e) A=0.15 M, B=0.2

The series of sub-figures contained within Figures 8 and 9 demonstrate the stability of the system for a variety of parameter values. The principal bifurcation parameters, f and H, are on the x and y axes, respectively. The line separating stable and unstable regions of parameter space indicates a bifurcation between stable and unstable steady states. Altering the system parameters A and B does little to affect the location of the bifurcation line in the *f-H* plane. This reinforces the notion that f and H should be treated as the principal bifurcation parameters, and that the system parameters A and B have a small effect on the stability of the CHD-BZ system. These parameters have a large effect on the dynamics of the system.

2.4 Modified Oregonator Dynamics

Our additions to the simple Oregonator model modify its dynamics and provide conditions for anomalous wave-velocity dispersion in an excitable reaction medium. The end result is a system that has what has been described (Szalai et al. (2003)) as non-monotonic relaxation of $[Br^-]$ to the steady state. As f and H are varied, various oscillatory and decaying $[Br^-]$ behaviors appear. Figure 12 shows a single excursion decay, featuring a "dip" in $[Br^-]$ following excitation as the system relaxes to the steady-state. Figure 13 shows an oscillatory (via a group of rapid oscillations) decay to the steady state. Figure 14 shows a complex limit cycle composed of quiescent periods separated by short periods of rapid oscillation. Figure 10 shows a diagram of these behaviors in *f-H* space. At very low f the steady-state is stable. At low and high values of f single excursion decay to the steady state is observed. At intermediate values of f both multiple oscillation decay to the steady state, and complex bursting oscillations are observed.

Figure 10: Map of Areas of Single-Excursion Decay, Complex Oscillations, and Multiple-Excursion Decay to the Steady-State as f and H are Varied

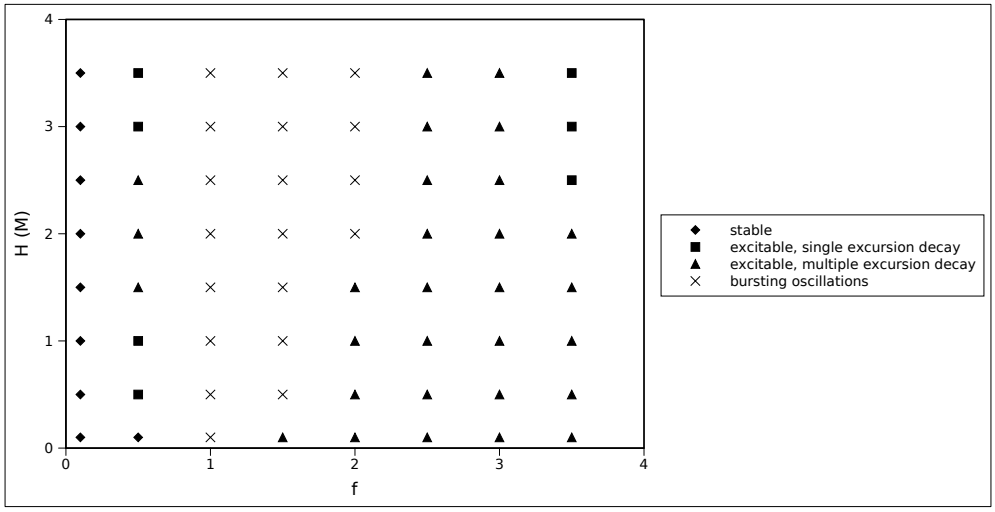

$A = 0.06$, $B = 0.02$, $g = 0.2$

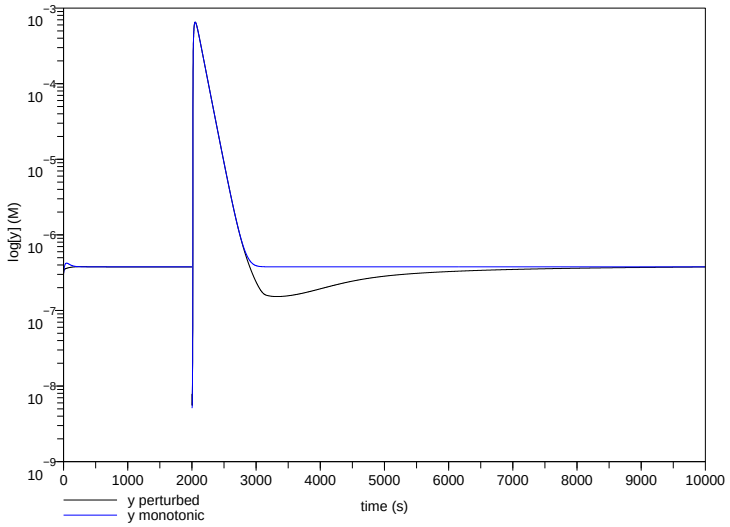

Figure 11: Monotonic and Non-monotonic Relaxation to the Steady State

Figure 12: Single Excursion Decay to the Steady-State

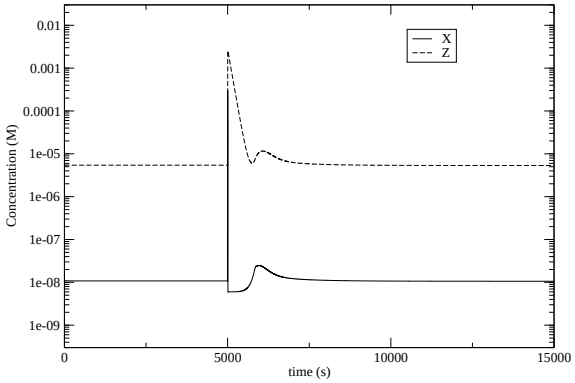

(a) Single Excursion X and Z

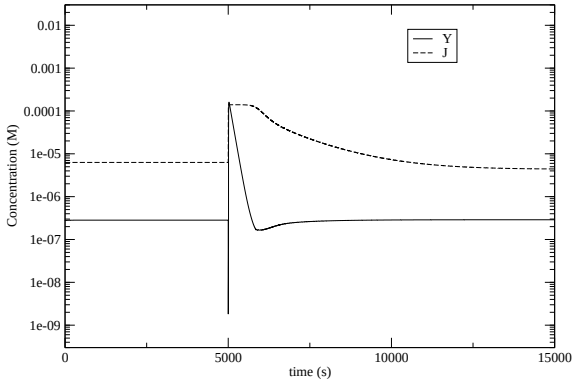

(b) Single Excursion Y and J

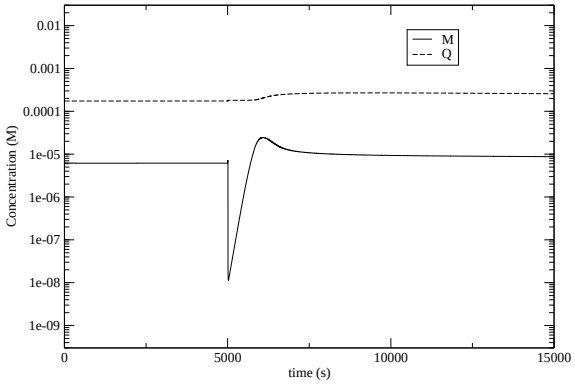

(c) Single Excursion M and Q

2.4.1 Single Excursion Decay to the Steady-State

Figure 11 shows the differences in character of [Br^-] recovery to the steady state in the simple Oregonator and the modified Oregonator. In both cases a small perturbation is applied to [Br^-] at $t = 2000$ s. The perturbation must be sufficient to move the system beyond a threshold in order to induce an excursion. Once an excursion has been initiated the system must traverse the limit cycle in order to return to the steady state. The monotonic blue line represents results obtained using the simple Oregonator where [Br^-] recovers monotonically to the steady-state. The black line represents results obtained using the modified Oregonator. The large dip in [Br^-] is the direct result of the reversible nature of reaction 7. The excursion is initiated by the $HBrO_2$ autocatalysis in reaction 4. As a result [Br^-] is produced rapidly via reaction 5, along with the intermediate species J. This in turn causes a second autocatalyis in reaction 6, which leads to rapid sequestration of [Br^-] in reaction 7_f in the form of the intermediate Q . The sequestration of Br^- causes its concentration to fall below that of the steady state. The slower process of reaction 7_r results in a slow recovery of bromide to the steady state from below. This non-monotonic recovery to the steady state is necessary for anomalous wave velocity dispersion in a quasi one-dimensional spatial system. Figure 12 shows the behavior of all six variables during non-monotonic decay to the steady-state.

In addition to non-monotonic recovery to the steady state, the modified model exhibits a variety of interesting temporal behaviors, some of which are described in experimental observations of the CHD-BZ oscillator (Hamik and Steinbock (2003); Ginn and Steinbock (2005); Manz and Steinbock (2006)).

2.4.2 Multiple Oscillation Decay to the Steady-State

The excitable region in the model exhibits a second form of decay, consisting of multiple oscillations while relaxing to the steady-state. Figure 13 shows the behavior

Figure 13: Multiple Oscillation Decay to the Steady-State

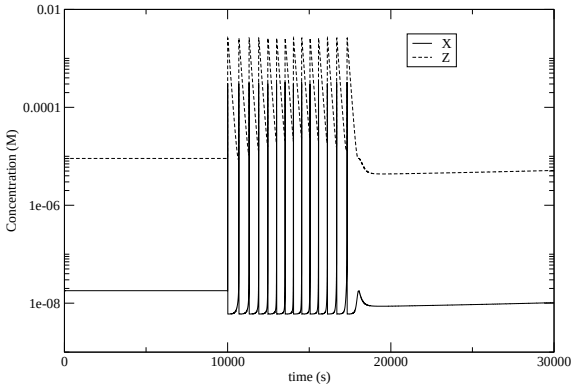

(a) Multiple Oscillatory Excursions, X and Z

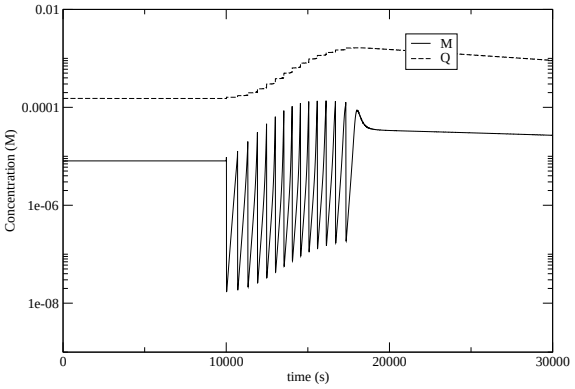

(b) Multiple Oscillatory Excursions, M and Q

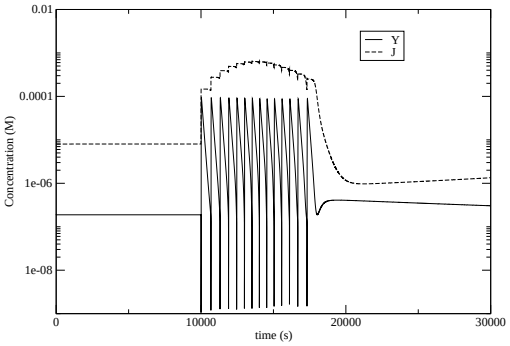

(c) Multiple Oscillatory Excursions, Y and J

of all six variables during such a relaxtion. The slow, compared to the single excursion case, accumulation of the intermediate Q during the oscillatory period eventually ends the multiple oscillation burst by the poisoning of Process B.

2.4.3 Complex Limit Cycle

The complex limit cycles seen here are composed of a quiescent period, followed by a period of oscillation, typically referred to as bursting (Janz et al. (1980)). Oscillations are initiated at the end of the quiescent period in the same manner as in the Oregonator. Process B becomes dominant here because [Br^-] is removed from the system by Process A. Process B also provides small amounts of intermediate J, which provides coupling to the additional reactions in the modified Oregonator. Both the difference between single excursion and multiple excursion decay, and the difference between multiple excursion decay and complex oscillatory decay is the level of accumulation of intermediate Q.

During a single cycle of the oscillation described above, reactions 6-8 also have an impact on the dynamics of the system. Our analysis agains starts with process B. The concentration of M is strongly affected via equilibrium 7 by the concentration of Y, via equilibrium 7. When Y is large, such as during process C, M is rapidly removed though 7_f. When Y is decreasing, such as during process B, reaction 1 competes favorably for Y, allowing [M] to increase as Q increases. In this way [Y] is accountable for rapid switching from 7_f to 6 during process C.

Process C is also responsible for the growth of the intermediate Q. During process C, an abundance of Y is formed, leading to a spike in the rate of 7_f. Although the increase in the rate of formation of Q is short lived, Q is not rapidly diminished. The equilibrium 7 lies to the right, and as a set of oscillations proceeds the [Q] increases. Eventually a critical [Q] is reached and new behavior is observed.

The species Q can act as a reservoir for Br^-. Although Reaction 7_r is slow, the

Figure 14: Complex Bursting Oscillations

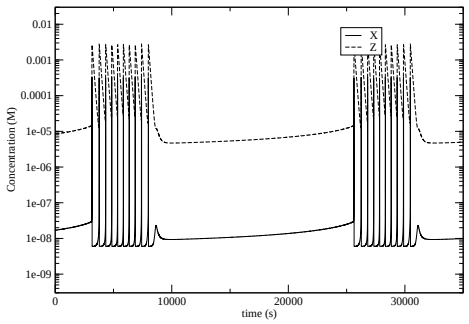

(a) Complex Limit Cycle, X and Z

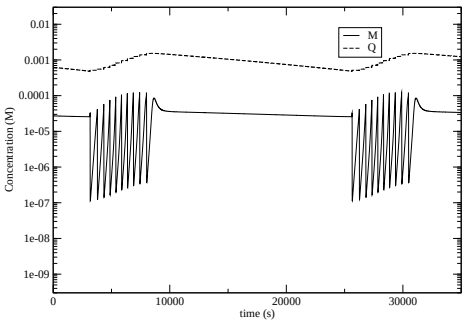

(b) Complex Limit Cycle, M and Q

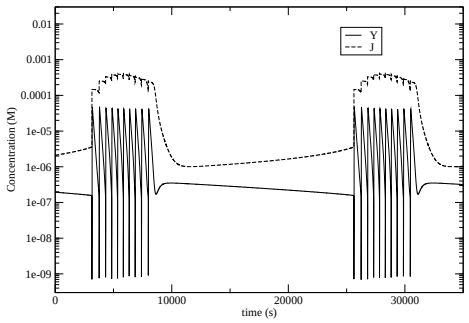

(c) Complex Limit Cycle, Y and J

relatively large [Q] makes it a significant independent source of Y during the removal of Y by process B. The result of a large [Q] is the inhibition of process A via Reaction 7_f. The switching between Process B and Process A occurs as [Y] reaches a critical concentration, below which autocatalysis of X becomes dominant. At the end of the oscillatory region of the limit cycle in a complex bursting oscillation, [Y] never reaches the critical point, and the system remains under the influence of process B.

The result of this interaction is the "dip" seen in [Y] in fig 14. The value of Y does reach a local minimum, and begins to rise because of the exhaustion of X and the presence of excess of Y caused by the large value of Q. The system can no longer oscillate as before due to the excess of Q. The long quiescent period is characterized by the removal of Q via reaction 7_r and the removal of M through the termination step reaction 8. Once [Q] has sufficiently declined, it no longer provides a large independent source of Y. Process A initiates and the oscillatory cycle can repeat.

2.5 Effects of Parameters on Model Dynamics

While the principal bifurcation parameters f and H determine the stability and overall dynamics of the modified Oregonator, the parameters A and B can be used to alter the dynamics. These parameters appear only in the Oregonator equations and thus they can be evaluated in terms of the Oregonator processes.

2.5.1 The Parameter A

The parameter A, corresponding to BrO_3^-, appears in reactions 2 and 4. Because A is a reactant in Processes A and B, it it is reasonable that it increases the speed at which these reactions proceed. This effect is seen as a decrease in the period of oscillation.

This effect is exhibited in figures 15 and 16. The frequency and number of oscillations increases as [A] increases. Parameter A appears in the rate constants of

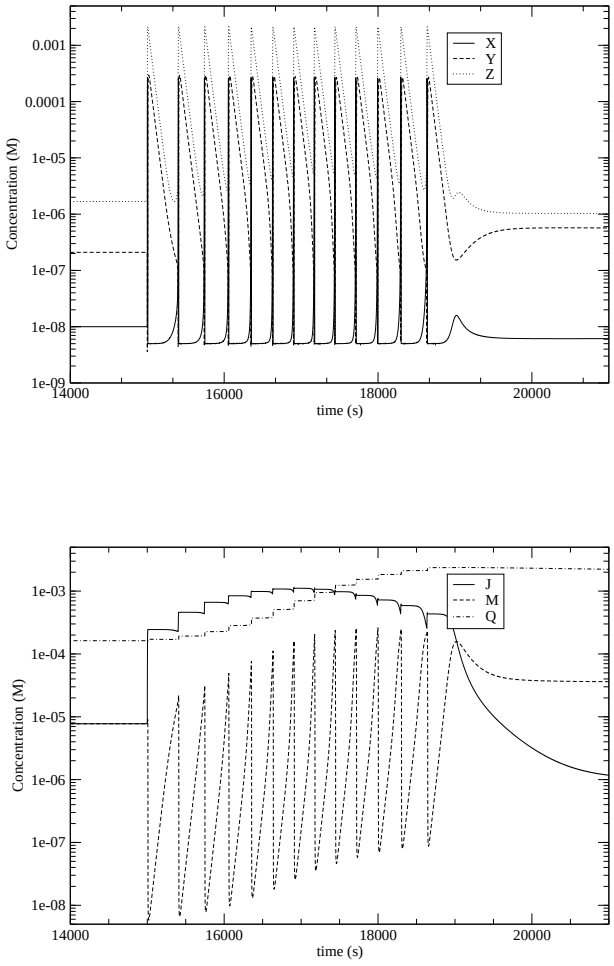

Figure 15: The Effect of Parameter A on Oscillatory Period, low A
A = 0.05, B = 0.05, f = 3.0, g = 0.2, H = 1.0

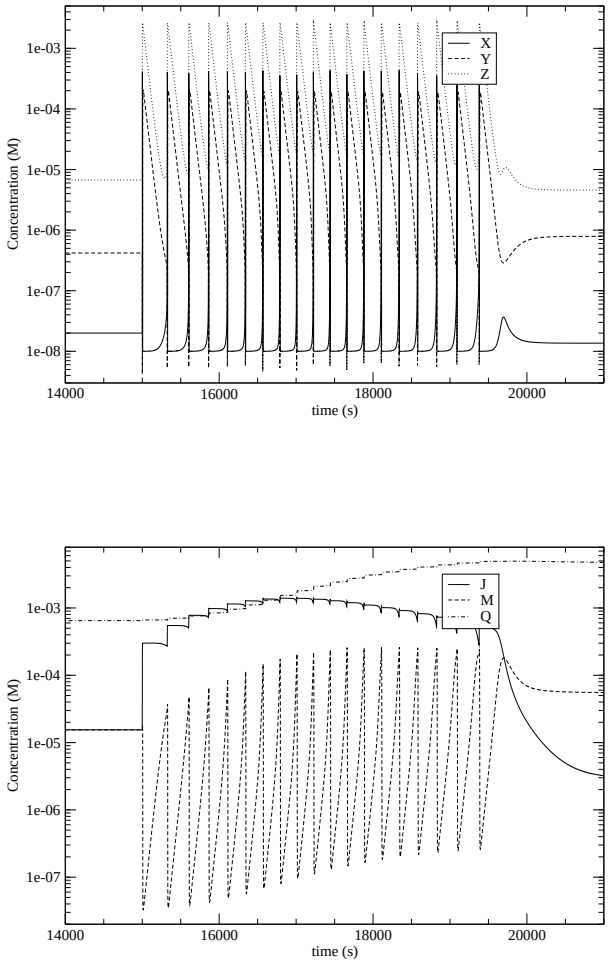

Figure 16: The Effect of Parameter A on Oscillatory Period, high A
A = 0.1, B = 0.05, f = 3.0, g = 0.2, H = 1.0

reactions 2 and 4. Increasing the value of A leads to an increase in reaction rate. In terms of the Oregonator, Process A and Process B are both affected. The increase in the rate of Reaction 2 speeds Process A, while the increase in the rate of Reaction 4 increases the rate of Process B. This is seen in the Modified Oregonator as the increased frequency of oscillation in the time periods shown in figures 15 and 16.

2.5.2 The Parameter B

The effect of the value [B] (B≡CHD) on the modified Oregonator is less pronounced than is the effect of A. Parameter B only appears in reaction 5, which is the basis of Oregonator Process C. An increase in B leads to an increase in the rate of reaction 5, which is the chemical process responsible for the recovery of [Br^-] in the oscillatory cycle. The result is a small decrease in the oscillatory period. Reaction 5 is also responsible for the production of Br^- in the recovery phase of the cycle. The presence of the stoichiometric factor f on the right-hand-side of reaction 5 further minimizes the effect of changes in the magnitude of B. A far more effective way to change the Br^- recovery rate is to alter f rather than B. Figures 17 and 18 show the increase in oscillation period that is obtained by increasing B.

2.6 The Effect of Equilibrium Reaction 7 on Modified Oregonator Dynamics

Reaction 7 of the modified Oregonator determines the relaxation of Br^- following perturbation of a near to steady-state system. The stability of the dip in [Br^-] is increased when [Q] is increased from its reaction 7 steady-state value. The behavior of the model was initially evaluated using $k_{-7} = 5.0e{-}4$. If reaction 7_r is slowed to $k_{-7} = 1.0e - 6$ [Q] remains nearly constant throughout oscillatory behavior. The steady-state [Q] is also significantly increased due to this change stabilizing the behavior of the entire model. The increased [Q] is responsible for greater production of Y

Figure 17: The Effect of Parameter B on Oscillatory Period, low B

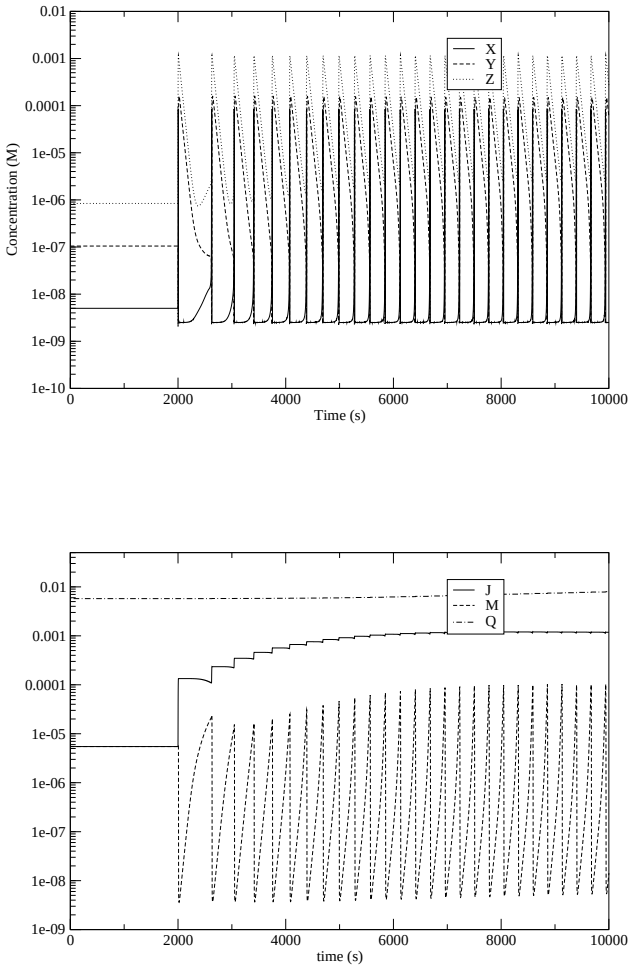

$A = 0.05,\ B = 0.05,\ f = 3.0,\ g = 0.2,\ H = 1.0$

Figure 18: The Effect of Parameter B on Oscillatory Period, high B

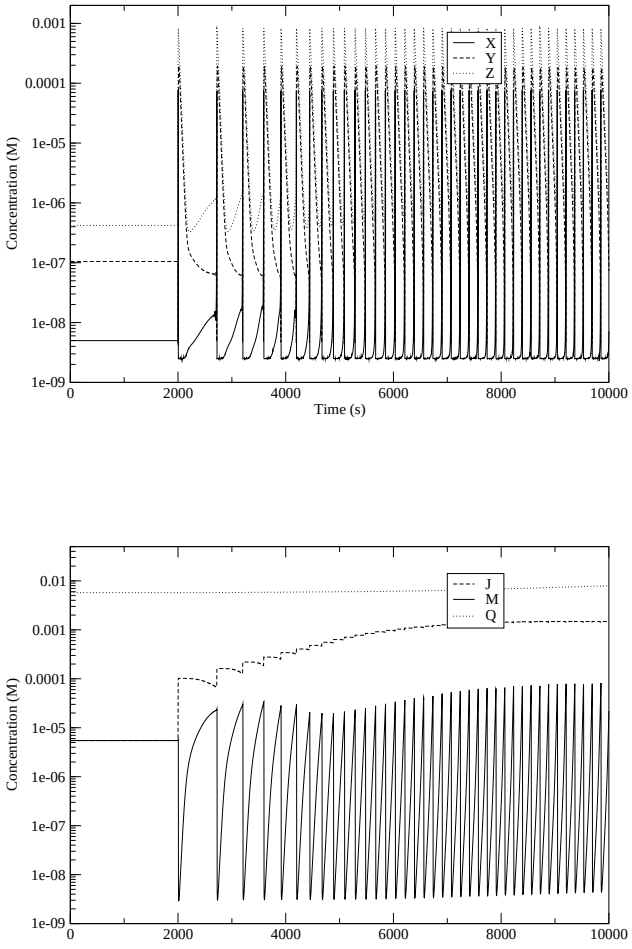

$A = 0.05$, $B = 0.1$, $f = 3.0$, $g = 0.2$, $H = 1.0$

Figure 19: Map of Areas of Excitability and Oscillation from the Steady-State

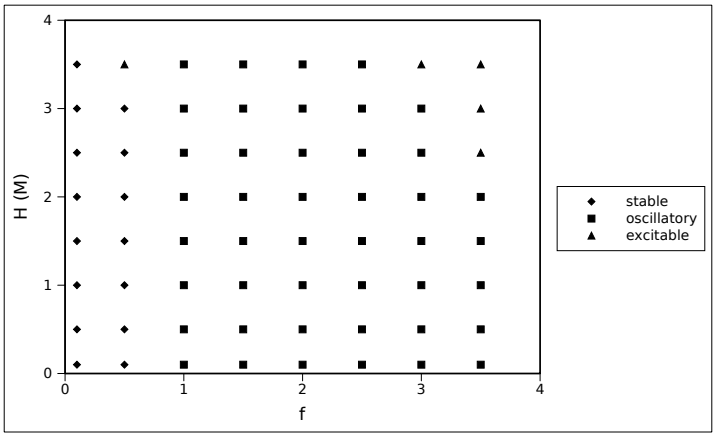

A=0.06, B=0.02, g=0.2

througout all phases of the modified Oregonator cycle. This change results in the loss of oscillatory bursts, as seen in figure 19. The minimization of bursting behavior afforded by the slower reverse rate in reaction 7 is advantageous in the study of traveling chemical waves in a quasi one-dimensional spatially distributed system.

2.6.1 Single Excursion Excitation in the modified Oregonator

The smaller rate constant k_{-7} allows for slightly different excitation dynamics. In Figure 20 a perturbation applied at t = 2000 s results in a single oscillatory excursion. The intermediate Q remains at a nearly constant concentration throughout the excursion. As in calculations using the faster k_{-7} a small decrease in the amount of Br^- results in Oregonator Process B becoming dominant. The relatively small change in the [Q] during an excursion makes it a candidate for removal as a dynamic variable. This would allow the model to be reduced to five variables, and would allow the use of Q as a useful parameter in the adjustment of the system to achieve stable wave propagation and dynamics in a quasi one-dimensional spatially distributed experiment.

When using the slower rate constant k_{7r} the system retains conditions in which a small perturbation to Br^- results in sustained oscillation. As in calculations done

Figure 20: Single Excursion

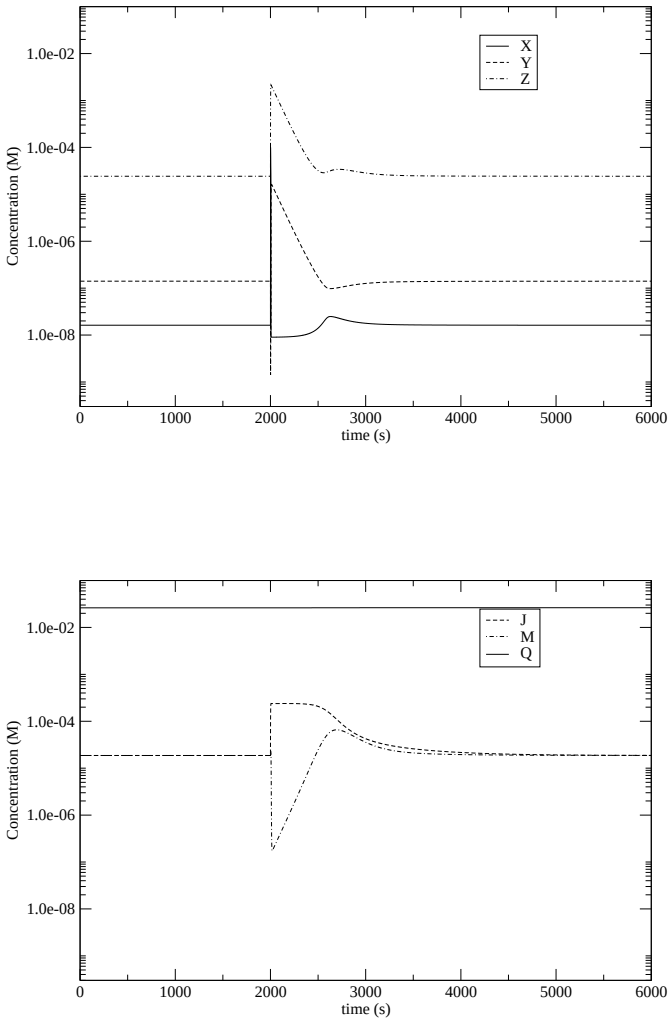

$A = 0.06,\ B = 0.02,\ f = 3.5,\ H = 3.0,\ g = 0.2$

Figure 21: Multiple Oscillations

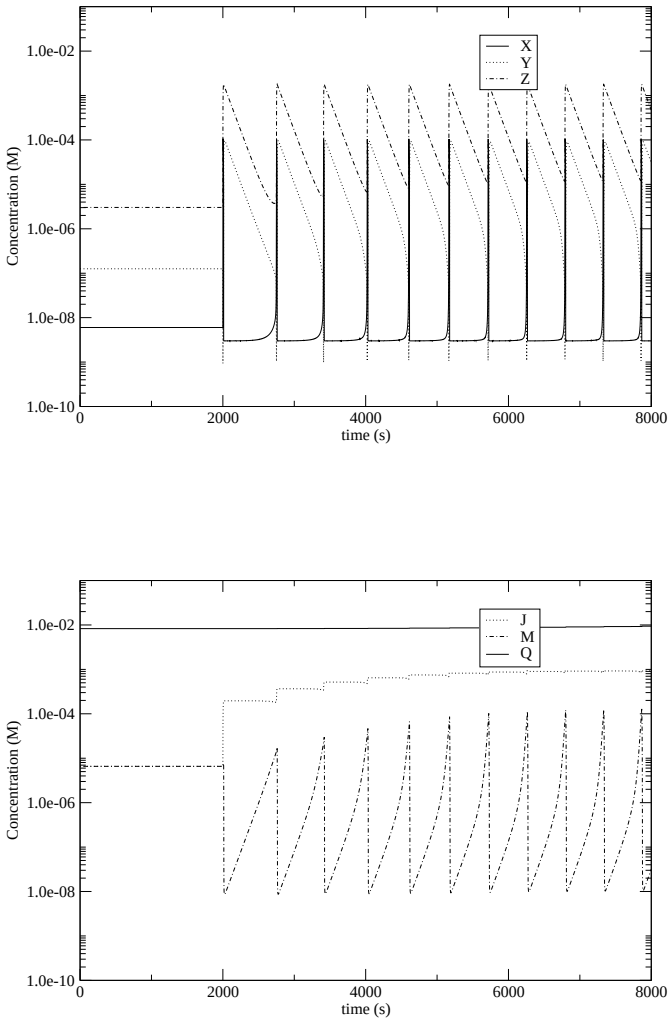

A=0.06, B=0.02, H=1.0, f=1.5, g=0.2

Figure 22: Termination of Oscillatory Excursion

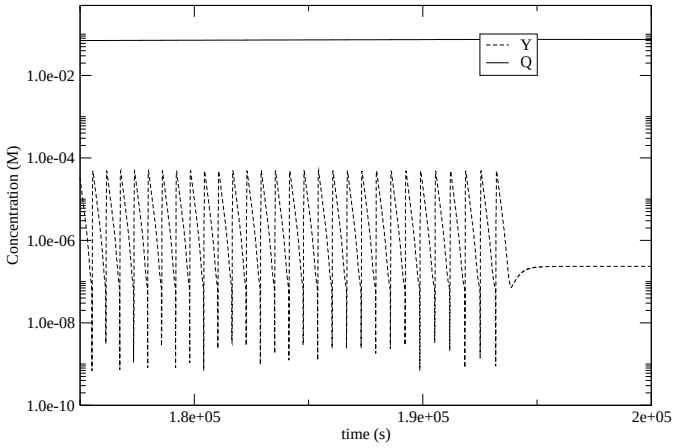

A=0.06, B=0.02, H=1.0, f=1.5, g=0.2

with the faster k_{-7} a small reduction in the concentration of Br^- results in Process B becoming dominant. In sustained oscillation the intermediate Q is far from equilibrium, and increases constantly for a long time period as seen in figure 15 . Eventually the concentration of Q reaches a critical point and the reverse of 7 is of sufficient magnitude to inhibit autocatalysis and force the return of the system to steady-state. This is in stark contrast to the single oscillatory excursion, where the concentration of Q reaches a critical point after only a single excursion, and highlights the problems that could be encountered if Q is removed from the system as a dynamic variable.

2.7 Dimensionless Equations

It is often convenient to rearrange differential equations into a dimensionless form. The primary advantage of doing so is simplification of the rate equations 9 and 10. The Tyson (Tyson (1982)) scaling of the Oregonator can easily be extended to the modified Oregonator. By making substitutions for the dynamic variables, the equations can be written in a dimensionless form which is often easier to work with. The following

substitutions are made:

$$\begin{array}{lll} X = \frac{k_4 Ax}{2k_3} & M = \frac{k_1 k_4 Am}{2k_3 k_{7f}} & \\ Y = \frac{k_4 Ay}{k_1} & Q = \frac{(k_4 A)^2 q}{2k_3 k_{7r}} & t = \frac{\tau}{k_5 B} \\ Z = \frac{(k_4 A)^2 z}{k_3 k_5 B} & J = \frac{k_4 k_{7f} Aj}{k_1 k_6} & C_0 = \frac{(k_4 A)^2 c0}{k_3 k_5 B} \end{array} \tag{11}$$

The scaled variables are proportional to the original variable, and are written as the lower case of the corresponding variable. The dynamic equations become dimensionless upon substitution of the new variables into the unscaled differential equations.

$$\begin{aligned} (\varepsilon)\tfrac{dx}{d\tau} &= \rho y - xy + x(1 - z/c0) - x^2 \\ (\varepsilon')\tfrac{dy}{d\tau} &= fz - xy + q - ym - \rho y \\ \tfrac{dz}{d\tau} &= x(1 - z/c0) - z \\ (\chi)\tfrac{dj}{d\tau} &= gx(1 - z/c0) - jm \\ (\psi)\tfrac{dm}{d\tau} &= jm - ym - q - \rho' m^2 \\ (\omega)\tfrac{dq}{d\tau} &= ym - q \end{aligned} \tag{12}$$

where

$$\begin{array}{lll} \varepsilon = \frac{k_5 B}{k_4 A} & \psi = \frac{k_1 k_5 B}{k_4 k_7 A} & \rho = \frac{2k_2 k_3}{k_1 k_4} \\ \varepsilon' = \frac{2k_3 k_5 B}{k_1 k_4 A} & \omega = \frac{k_5 B}{k_8} & \rho' = \frac{k_9 (k_1)^2}{k_3 (k_7)^2} \\ \chi = \frac{2k_3 k_5 k_7 B}{k_1 k_4 k_6 A} & & \end{array}$$

Numerical values for the scaling constants are obtained by using typical values of the parameters: $A(0.06)$, $B(0.02)$ and $H(1.0)$, and rate constants in Table 1, and the value $k_{7r} = 5.0e - 6$.

$$\begin{array}{lll} \varepsilon = 1.19x10^{-2} & \psi = 9.52 & \\ \varepsilon' = 5.4x10^{-6} & \omega = 5.0x10^{4} & \chi = 3.83x10^{-3} \end{array}$$

The value of the scaled differential equations is their relatively simple form. Scaled equations may be easier to work with, e.g., when solving the differential equations for fixed solution points or steady states. In some cases with proper scaling the stiffness of the set of equations is also decreased, yielding faster integration times when extended into a quasi one-dimensional spatially distributed model. One is also able to define the dimensionless constants ε, ε', χ, ψ, and ω in such a way to separate the time scales that the dimensionless variables move on. If one of the dimensionless constants multiplies a rate term, i.e., $(\omega' \frac{dq}{d\tau})$, is sufficiently smaller in magnitude than similar terms, that variable can be removed from the system via the steady-state approximation, $(\omega' \frac{dq}{d\tau}) = 0$.

2.8 Five-Variable Model

The numerical value of ω is much greater than that of the next largest coefficient, ψ, resulting in the rate of change $\frac{dq}{d\tau}$ being much smaller than the other rates of change. This allows the use of a steady state approximation for the variable q, allowing a subsequent reduction to a five variable system of differential equations.

$$\begin{aligned}
(\varepsilon)\frac{dx}{d\tau} &= \rho y - xy + x(1 - z/c0) - x^2 \\
(\epsilon')\frac{dy}{d\tau} &= fz - xy - \rho y \\
\frac{dz}{d\tau} &= x(1 - z/c0) - z \\
(\chi)\frac{dj}{d\tau} &= gx(1 - z/C_0) - jm \\
(\psi)\frac{dm}{d\tau} &= jm - p'm^2
\end{aligned} \tag{13}$$

This set of five dimensionless differential equations 13 is expected to reasonably reproduce the behavior of the six-variable model. However, the five-variable reduced model behaves significantly different from the original six-variable case. Figure 25 shows behavior at various values of the parameters f and H. The areas of primary interest are excitable and oscillatory conditions. The five-variable model is used

Figure 23: Scaled Model, Oscillations

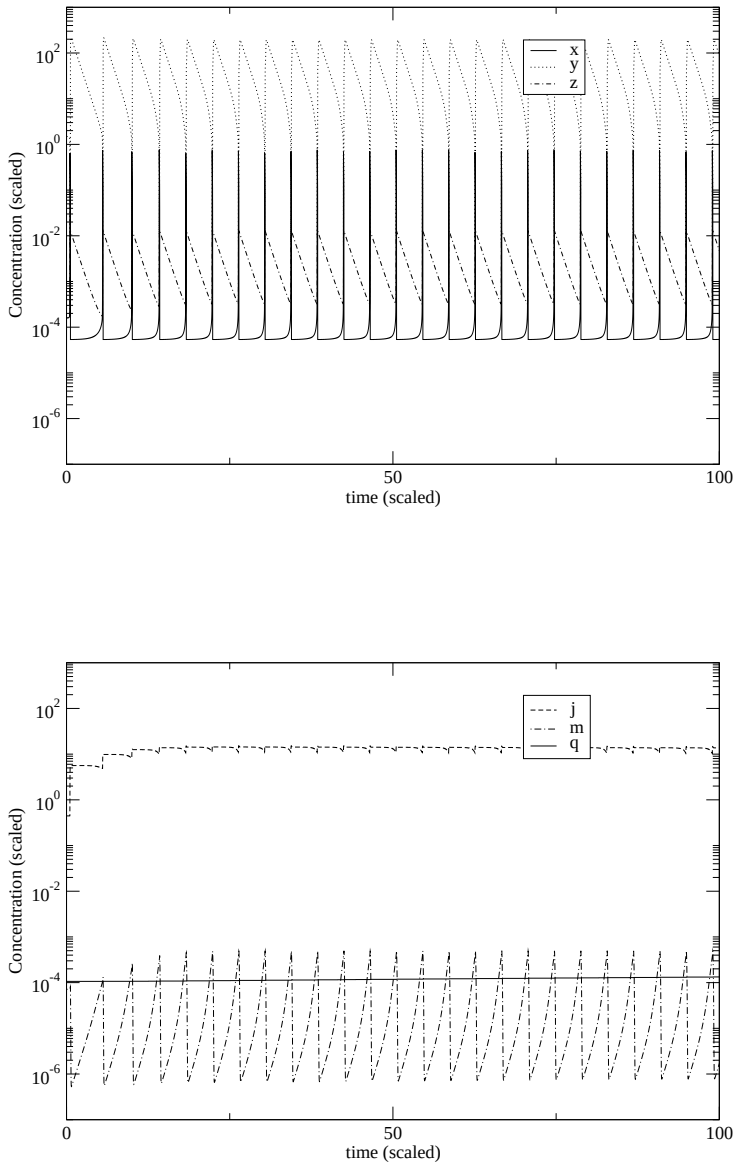

A=0.06, B=0.02, H=2.5, f=2.0, g=0.2

Figure 24: Scaled Model, Excitation

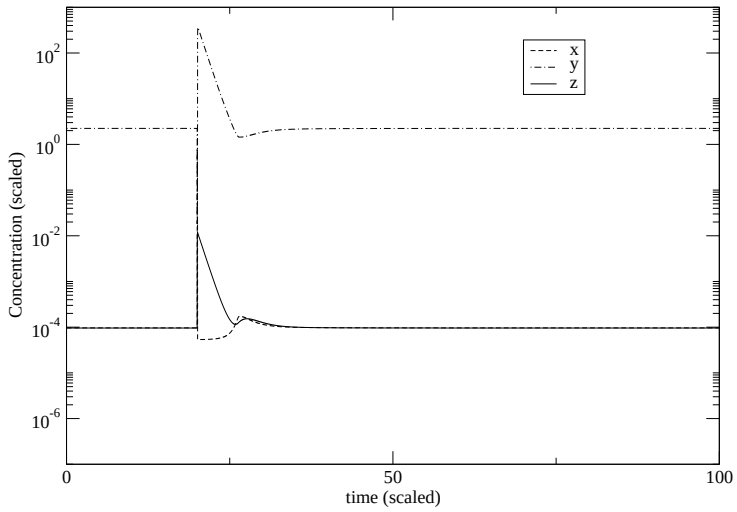

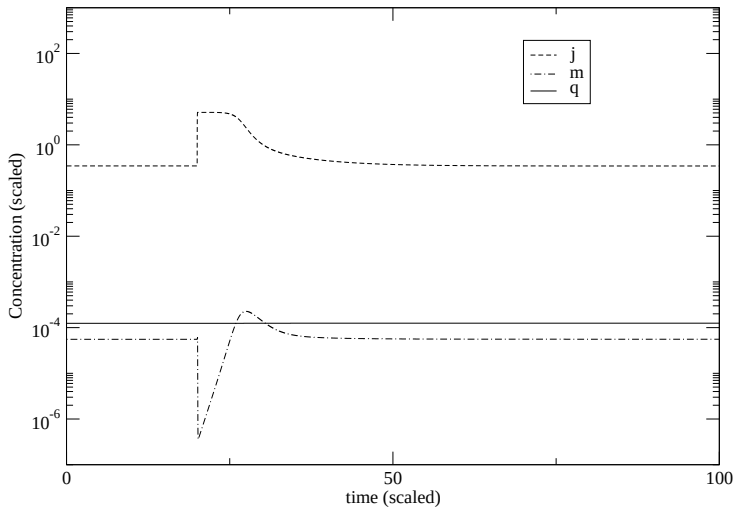

A=0.06, B=0.02, H=2.5, f=3.5, g=0.2

Figure 25: Stability of the Reduced Model While Varying Parameters f and H

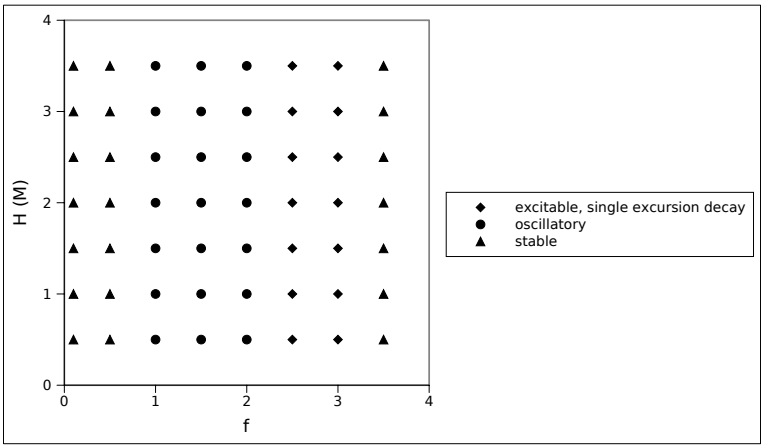

A = 0.06, B=0.02, g=0.2

with the smaller value for the rate constant $k_{7r} = 5.0x10^{-6}$, as a result no multiple oscillatory relaxations to the steady-state are observed for excitable conditions.

2.8.1 Oscillations

Oscillations are seen in the five-variable model for the conditions seen in figure 25. The five-variable model qualitatively reproduces some of the features of the six-variable modified Oregonator. The elimination of q as a dynamic variable affects the dynamics of the variables j, y, m during oscillatory behavior, while the dynamics of the species x and z are largely unaffected. Figure 26 shows changes in behavior of the five-variable model due to the elimination of q as a dynamic variable. The magnitude of variable m decreases significantly, and the oscillations in j change character. With the large decrease in magnitude of m, j becomes completely controlled by Process B. This is seen as the spikes in j and x, both occurring during the autocatalytic reaction 4. Autocatalysis of m in reaction 6 is not pronounced, because of the relatively small magnitude of m, plus the second-order removal of m in reaction 8 prevents any large increases in magnitude.

Figure 26: Oscillations in the Five-Variable Model

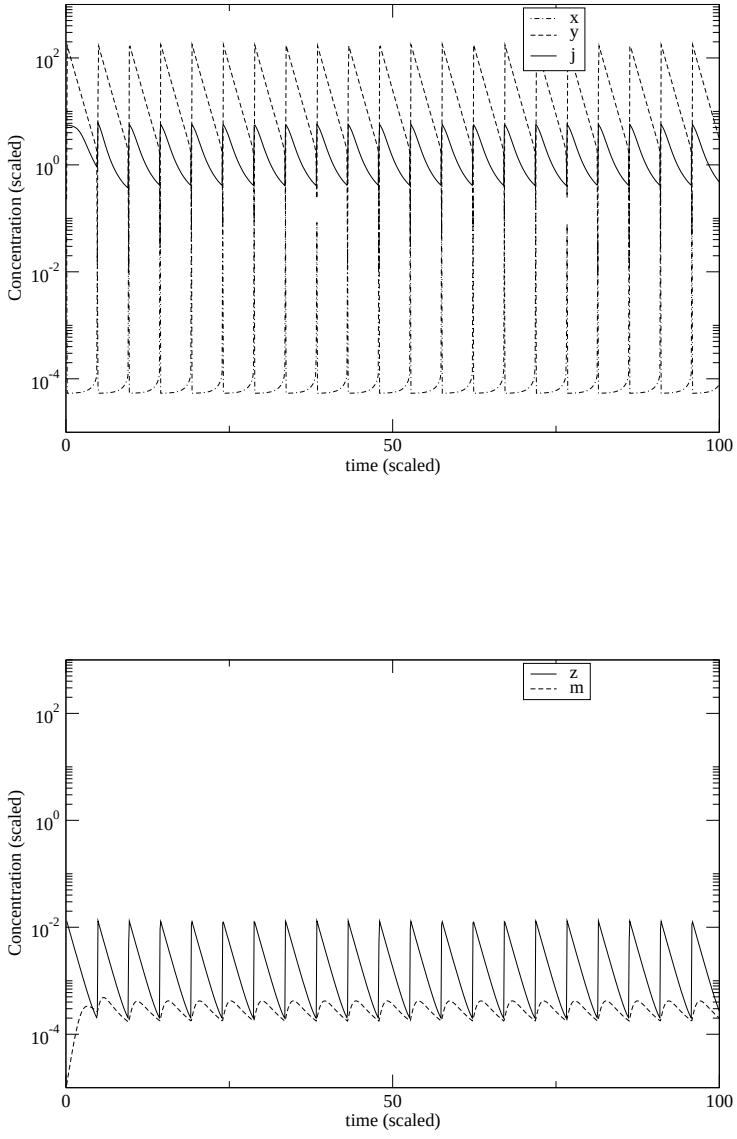

A=0.06, B=0.02, H=2.5, f=1.5, g=0.2

2.8.2 Excitability

The five-variable model also exhibits excitability from the steady state. However, there is a large difference in the dynamics of the system. Non-monotonic relaxation to the steady state is no longer observed in y, but appears in j, and to a lesser extent in m. Excitation is obtained through a small instantantaneous decrease to the magnitude of y, which is sufficient to initiate Process B. When autocalatylis of x ends the system returns to equilibrium through Process A. During relaxation to the steady state j is removed through the slow autocatalysis in Reaction 6. The peak magnitude of m is delayed compared to that of x, y, and z. The autocatalytic production of m is responsible for the removal of j, causing the drop in magnitude of j below its steady state concentration. The overall dynamics of the system, seen in figure 27, is greatly changed from that of the six-variable model. The model reduction removes the dip in $[Br^-]$, and the five-variable system does not exhibit anomalous wave-velocity dispersion.

Figure 27: Excitation from the Steady State in the Five-Variable Model

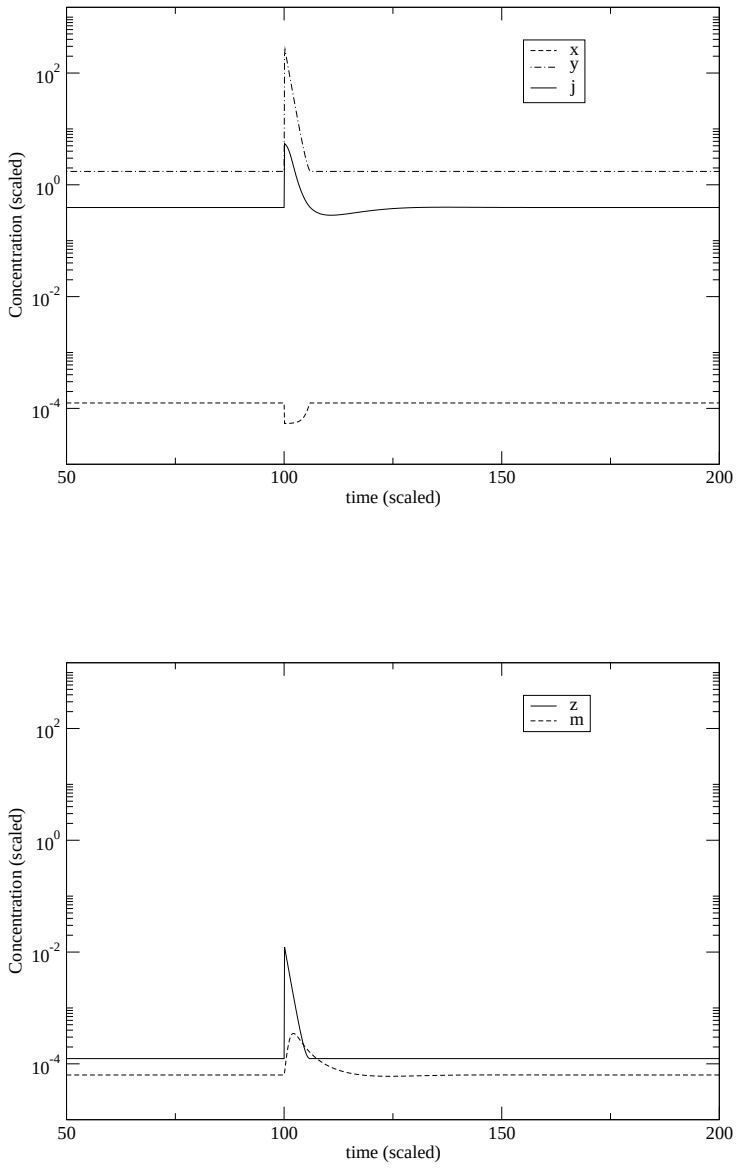

A=0.06, B=0.02, H=2.5, f=2.5, g=0.02

3 Travelling Waves in the Modified Oregonator

3.1 Flux Terms

The well-stirred modified model can be extended, by use of Fick's second law, to a quasi one-dimensional spatially distributed system analogous to the thin capillary tube (Hamik and Steinbock (2003); Manz and Steinbock (2006); Bordyugov et al. (2010)). A grid of points is constructed in one spatial dimension, each point containing the temporal chemical dynamics of the six non-linear differential equations. Each differential equation contains an extra term to describe the flux between adjacent points. The flux term takes the form of Fick's second law of diffusion, where c is the concentration of the chemical species, D is the diffusion coefficient, and l is spatial distance.

$$\frac{\delta c}{\delta t} = \frac{\delta}{\delta l} D \frac{\delta c}{\delta l} \tag{14}$$

This equation describes the diffusive change in concentration at a point in terms of the second dericative of the concentration gradient at that spatial point. In this work the second derivative is numerically approximated by equation $\frac{\delta c}{\delta t} = (D/l^2)[c_{i+1} + c_{i-1} - 2(c_i)]$, where i is the grid point at which the flux is desired; i+1 and i-1 are adjacent grid points.

The diffusion coefficient used for all chemical species is $1\text{x}10^{-5} cm^2\ s^{-1}$, which is a default value used for small molecules in dilute aqueus solution (Field and Noyes (1974b)). The spacing between grid points (l) is 0.04 cm.

The end result is a set of six partial differential equations, representing both the reactive and diffusive processes occurring.

$$
\begin{aligned}
\frac{dX}{dt} &= -R1 + R2 - 2.0R3 + R4 + \frac{\delta X}{\delta t}_{flux} \\
\frac{dY}{dt} &= -R1 - R2 + \frac{1}{2}fR5 - R7_f + R7_r + \frac{\delta Y}{\delta t}_{flux} \\
\frac{dZ}{dt} &= 2.0R4 - R5 + \frac{\delta Z}{\delta t}_{flux} \\
\frac{dJ}{dt} &= gR4 - R6 + \frac{\delta J}{\delta t}_{flux} \\
\frac{dM}{dt} &= R6 - R7_f + R7_r - 2.0R8 + \frac{\delta M}{\delta t}_{flux} \\
\frac{dQ}{dt} &= R7_f - R7_r + \frac{\delta Q}{\delta t}_{flux}
\end{aligned}
\tag{15}
$$

These equations are integrated using LSODES (Hindmarsh (1980)) with a varying number of gridpoints, depending on the requirements of the individual calculation.

3.2 Anomalous Wave-Dispersion

Anomalous wave-velocity dispersion relationships in one and two quasi-dimensions have been experimentally identified in the CHD-BZ reaction (Hamik and Steinbock (2003); Manz and Steinbock (2006); Bordyugov et al. (2010)). A normal dispersion relationship is described as a series of traveling waves proceeding at a constant velocity, c_0 and at a characteristic distance, λ_0, between consecutive waves (fig. 1). The original observation of traveling waves of chemical activity in the ferroin-catalyzed BZ system (Zaikin and Zhabotinskii (1970)) was made in a quasi two-dimensional system consisting of a thin layer of reagent in a petri dish. The waves appeared as an expanding target pattern surrounding an initiating center. A quasi one-dimensional system may be thought of as movement along a straight line passing through the initiating center. In a system with normal dispersion a wave initated at a distance less than λ_0 behind a preceeding wave will fall behind that wave until it reaches the distance λ_0 and is traveling at the velocity c_0. In a quasi one-dimensional system this behavior appears as a series of waves of chemical activity starting at the initiation center and moving down the line with uniform spacing and velocity.

In anomalous wave velocity dispersion there exists a distance, λ_{max}, between consecutive chemical waves below which a secondary wave arising at the initiation center travels at an increased velocity with relation to the primary wave. If the secondary wave is located at a distance greater than λ_{max}, it travels at an identical velocity to that of the primary wave. Various behaviors have been observed experimentally when a second wave is initiated at an interpulse distance less than λ_{max}. Depending upon experimental conditions the CHD-BZ oscillator exhibits wave stacking, where chemical waves travelling in the wake of the primary wave stack up behind it, much like cars delayed behind a slow driver. Chemical waves are also observed to merge with the leading pulse, as well as initiate new pulses upon interacting with the wake of a leading wave.

3.3 Mechanism of Wave Propagation

Travelling waves in a BZ system are generally studied in a region where the chemical steady-state is stable, but is excitable. This is similar to conditions in the well-stirred model where a perturbation results in a single oscillatory excursion (Field and Troy (1979)). A threshold exists that determines the behavior of the system after the application of a perturbation. Any perturbation below the threshold will result in a rapid return to the steady state, while a perturbation that exceeds the threshold requires a complete traverse of the limit cycle to return to the steady state. In the calculations described here all perturbations applied to the modified Oregonator are instantaneous decreases to $[Br^-]$.

Pulses travel through the excitable medium as a chemical excitation wave. The pulse is initiated through Process B, the autocatalytic generation of $HBrO_2$, which causes an increase in oxidized catalyst. The front travels through the excitable media as an oxidation wave. Ahead of the chemical wave $HBrO_2$ diffuses from the pulse into the area directly in front of it, causing a decrease in $[Br^-]$ via reaction 1. As $[Br^-]$

ahead of the front is depleted the autocatalytic process B moves forward through space. If the steady state is maintained in the direction of wave propagation, the pulse will travel through the excitable medium at constant velocity.

The concentrations of intermediate species returns to the reduced steady state behind the pulse. A maximum in [ferroin] and [Br^-] follows directly behind the pulse of $HBrO_2$. The profile of the wake is similar to the relaxation of an oscillatory excursion to the steady-state in the well-stirred model, as in fig. 12. [Br^-] falls to a level below the steady-state before recvovery from below. This is the behavior described previously (section 2.4), and is a necessary feature for development of anomalous wave velocity dispersion.

The standard Oregonator model produces travelling wave patterns with a normal dispersion relationship. The interpulse distance is determined by [Br^-] in the wake of the excitation pulse. The trailing end of a travelling wave has [Br^-] greater than that of the steady state. This elevated [Br^-] is inhibitory to the propagation of a second wave. Any excitation wave found in this region will be subject to inhibition of its movement and will collapse or travel at a reduced velocity until it has reached an interpulse distance where the elevated concentrations behind the pulse have returned to the steady state.

3.4 Single Waves

3.4.1 Wave Initiation From Steady-State Concentration

Traveling chemical waves are obtained by applying a perturbation, an instantaneous reduction of [Br^-], to the modified Oregonator equations in a region where the dynamics are excitable, but not spontaneously oscillatory. Regions where the system is excitable to oscillation can also be used if the slowly changing [Q] is sufficiently far from its steady-state value to prevent oscillation, but retains single excursion excitability. The perturbation causes the reaction dynamics to be controlled by process

B. NMR studies (Britton (2003)) of the CHD-BZ system have successfully measured the speed of traveling waves, as have studies in thin capillary tubes (Hamik and Steinbock (2003)). In the calculations presented here, waves are initiated at a zero-flux boundary condition to ensure propagation in only one direction.

Figure 28 provides a close view of the concentrations of the dynamic variables in the wave front; the wave is traveling from left to right into an excitable steady-state medium. The x-axis in this figure shows the spatially coupled points in the quasi one-dimensional system. The decrease in [Y], which initiates wave propagation, is clearly visible at the leading edge of the chemical wave. Autocatalytic production of [X], and its rapid removal, are also visible directly behind the wave front.

Figure 29 provides a wide view of the same traveling wave shown in fig. 28. Visible here is the recovery of the chemical species in the wake of the traveling wave. The non-monotonic recovery of Y to the steady state is clearly visible at ~50 cm. This feature coincides with small peaks in M and X, and a small valley to peak transition in Z. These features are the result of the augmented Process C in the modified Oregonator. In the wake of the chemical wave there is initially a large amount of J remaining from Process B. This is involved in a slow auto-catalysis with M, which in turn aids in the removal of Y through reaction 7_f. The removal of Y causes Process B to begin to compete favorably here, although the critical point for transition from Process A to Process B is never reached, and Process B never becomes dominant. The constant production of Y via reaction 7_r is responsible for the retardation of Process B in this situation. The result of the competition between Processes A and B is an unstable region contained within the the non-monotonic recovery (dip) of Y to the steady state, seen in fig. 29 between ~30 cm to ~50 cm. This is the area in which all anomalous wave velocity is observed.

Figure 28: Travelling Wave Front Propagation in an Excitable Medium

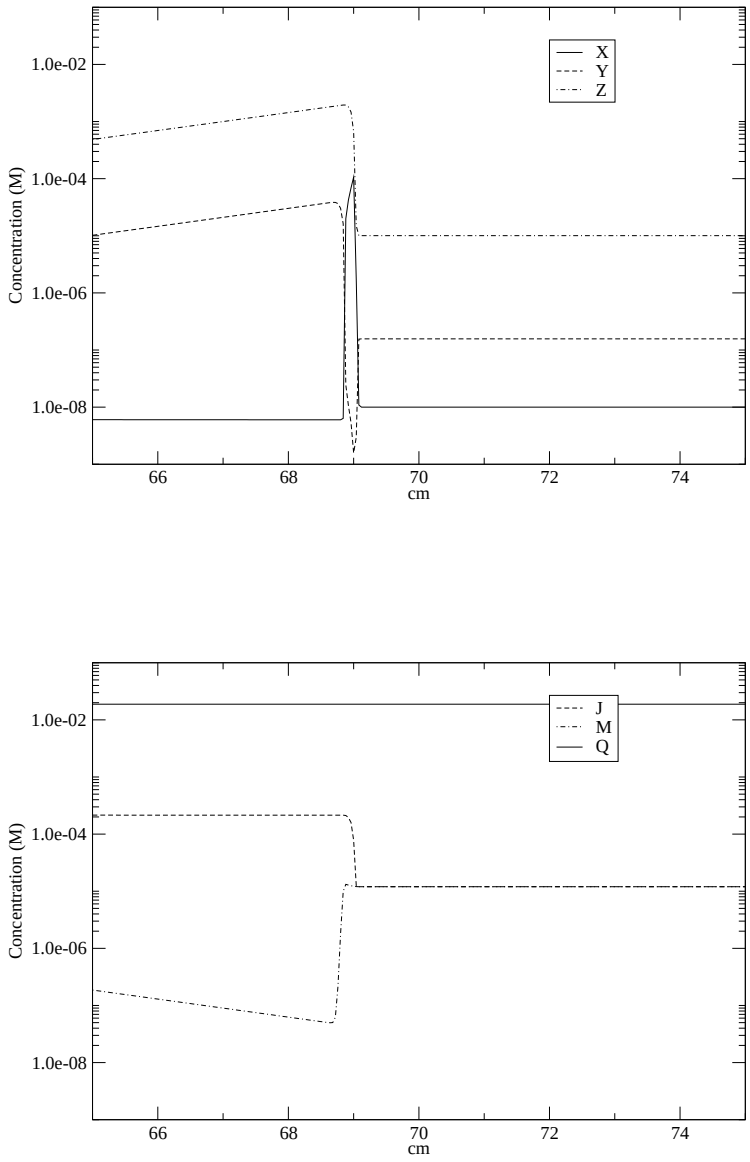

A=0.06 M, B=0.02 M, H=2.0 M, f=4.0, g=0.2

Figure 29: Travelling Wave Propagation in an Excitable Medium

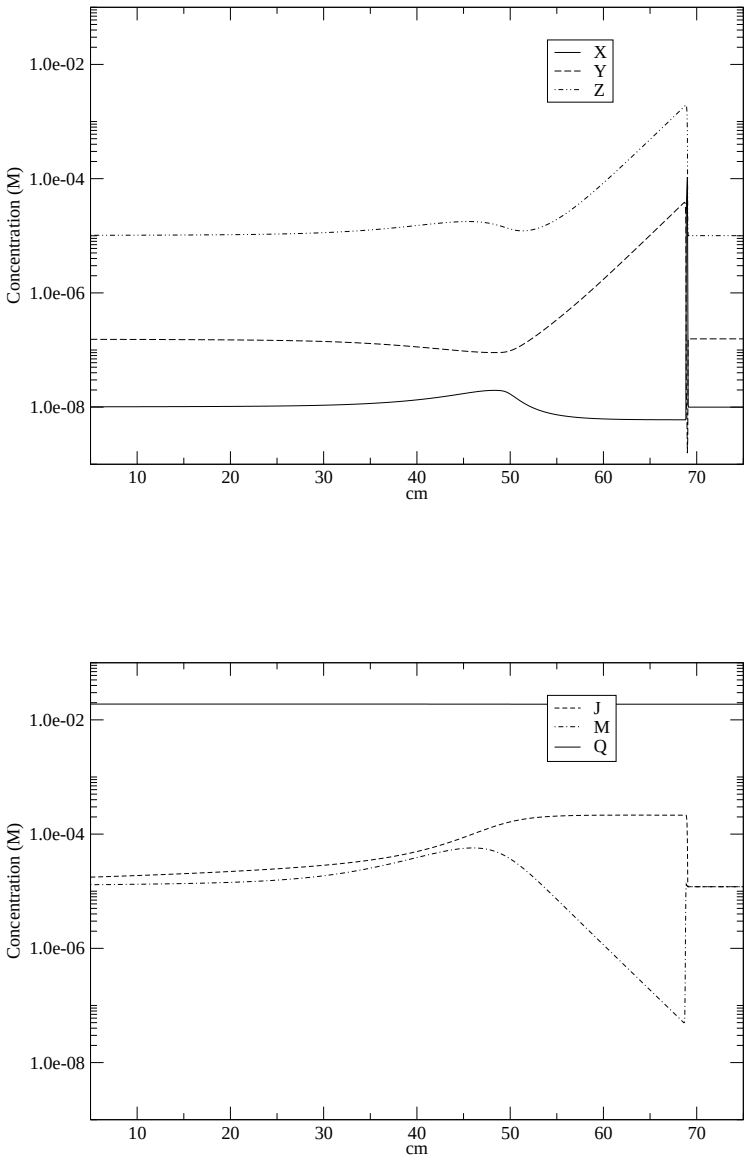

A=0.06 M, B=0.02 M, H=2.0 M, f=4.0, g=0.2

3.4.2 Dynamic Control of the Wake Via Parameters A, B, and the variable Q

The magnitude of the dip in [Br^-] present in the wake of a traveling chemical wave is the primary feature affecting anomalous wave dispersion in a quasi one-dimensional spatially distributed system. The instability introduced by diffusive coupling through space occasionally causes unexpected results in regions where the well-stirred model predicts excitable behavior. This is perhaps analogous to the diffusive spatial destabilization of a spatially homogeneous system leading to the formation of a Turing structure (Turing (1952)). Altering the parameters A and B allows control of the dynamics of the system to ensure traveling waves appear.

3.4.3 Parameter B

Figure 30 shows the effect of varying parameter B on the dynamics of [Br^-] in a traveling chemical wave. While parameter A is also changed in these figures, the magnitude of the effect is much smaller than for changes in B, and can be neglected. The primary change to the waveform visible in the figure is the broadening of the Br^- wave as [B] is decreased. This is a direct result of B appearing only in Process C. If [B] is greater, R5 increases, resulting in a faster relaxation to the steady state, and decrease in breadth of the chemical wave.

3.4.4 Parameter A

Parameter A has little effect on the [Br^-] dip. Parameter values are identical in figures 32a and 32b except for A. The shape of [Br^-] is nearly identical, which should be expected because small changes in A will result in only small changes in the rate of reaction 2. The values of A used in this work are purposefully kept small to avoid excessive removal of Br^- via reaction 2.

Figure 30: The Effect of Parameter B on [Br^-]

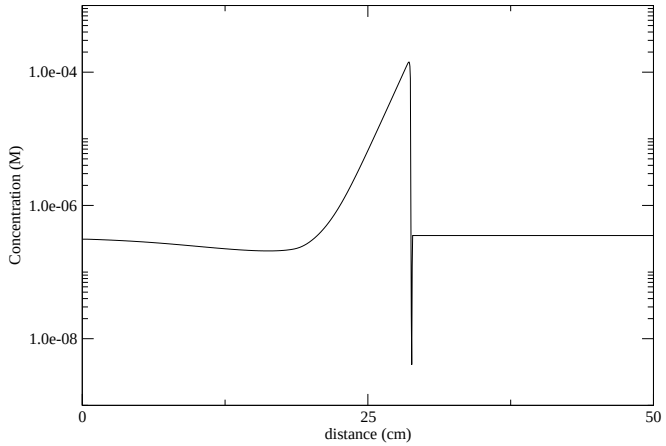

(a) A=0.15 M, B=0.05 M, H=1.0 M, f=3.5

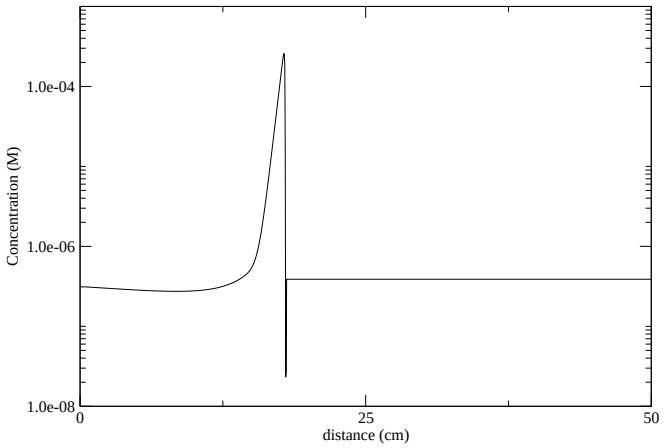

(b) A=0.2 M, B=0.2 M, H=1.0 M, g=0.2 f=2.7

Figure 31: The Effect of Parameter A on [Br^-] "dip"

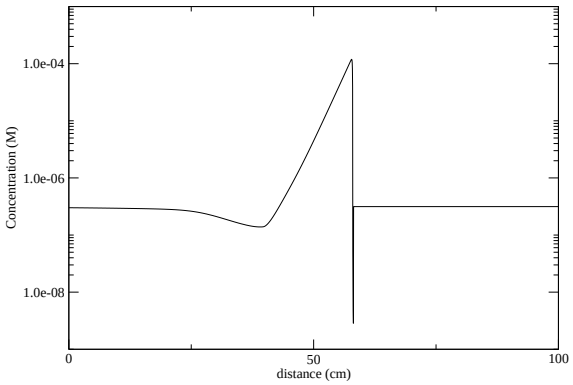

(a) $A = 0.1$ M $B = 0.02$ M, $H = 1.0$ M, $g = 0.2$, $f = 5.0$

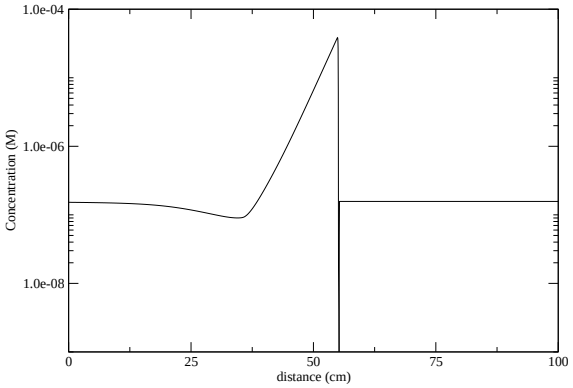

(b) $A = 0.06$ M, $B = 0.02$ M, $H = 1.0$ M, $g = 0.2$, f =5.0

3.4.5 Treating [Q] as a Model Parameter

Although Q is a dynamic variable in the modified Oregonator, it can be useful to consider [Q] as a parameter to affect the stability of the quasi one-dimensional system. The scaling and model reduction of equations 13 suggests [Q] as a candidate for model reduction through the steady-state approximation, because the reverse reaction 7 is very slow. By supplying an initial condition $[Q]_0$ that is far from its steady-state concentration one can affect the stability of the quasi one-dimensional system through the size of the $[Br^-]$ dip. An increase in [Q] results in a significant increase in $[Br^-]$ during all model Processes. Figure 32 shows the difference in character of the $[Br^-]$ dip in conditions where [Q] initially lies at the steady state, and where it has been increased. Although the parameters A, B, H, and g are identical in the example, the parameter f must be varied to obtain conditions where the system is excitable to a single excursion. The very high value for f (6.5) is necessary for excitability in conditions where [Q] lies at the steady state, while a much lower value for f can be used if $[Q]_0$ is far from the steady state. This is not unexpected, because [Q] has a large role in Br^- production. Altering $[Q]_0$ is merely an alternate method of affecting Br^- and changing the stability of the system.

3.5 Multiple Traveling Chemical Waves

It is possible by applying a second perturbation to Y in the wake of a traveling chemical wave to observe the dynamics of multiple chemical waves in the quasi one-dimensional spatially distributed system. The presence of multiple waves allows the study of anomalous velocity dispersion.

3.5.1 Anomalous Velocity Dispersion in a Pair of Chemical Waves

Figures 33 and 34 show in different formats the same pair of chemical waves traveling through an excitable medium. Figure 33 is a time-space plot, where the lines in the

Figure 32: The Effect of [Q] on [Br^-] "dip"

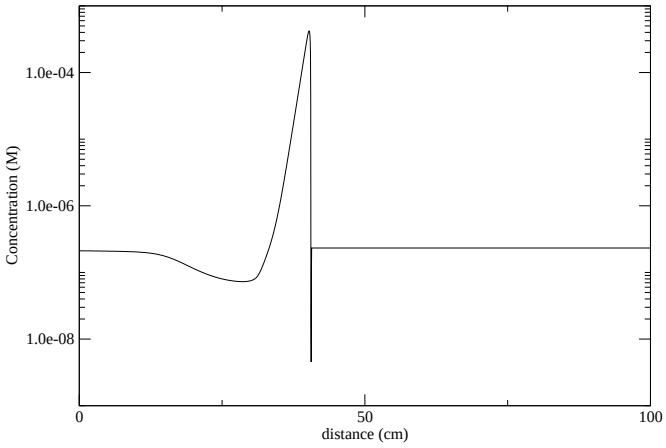

(a) $A = 0.06$ M, $B = 0.02$ M, $H = 0.5$ M, $g = 0.2$, $f = 6.5$, $[Q]_{steadystate} = 0.0038$ M

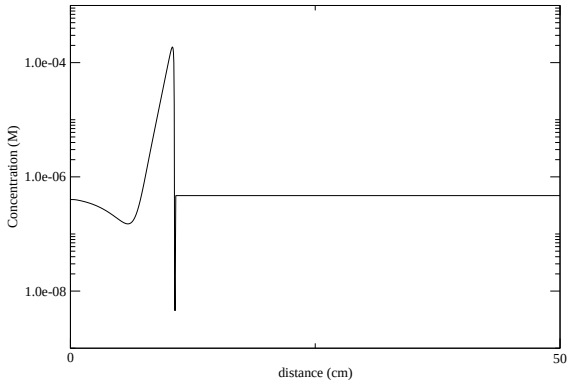

(b) $A = 0.06$ M, $B = 0.02$ M, $H = 0.05$ M, $g = 0.2$, $f = 2.1$, $[Q]_0 = 0.096$ M

Figure 33: Two Traveling Chemical Waves Exhibiting Anomalous Velocity Distribution

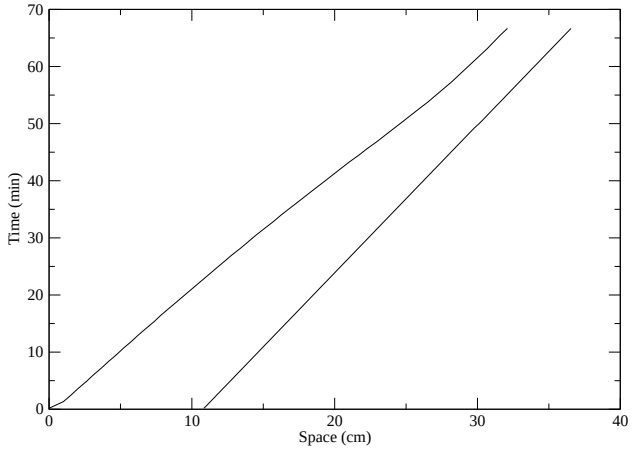

A=0.06 M, B=0.02 M, H=0.5 M, g=0.2, f=2.1, $[Q]_0$=0.09 M. The initial interpulse distance is 11 cm.

body of the plot represent the front of a chemical wave. The x-axis is the distance from the origin, and the y-axis is total time elapsed. The inverse slope of the line at any point is the velocity of the wave front in cm/min at that point. The figure clearly shows the approach of the second chemical wave to the first, and the accompanying increase in propagation velocity. As the second wave reaches the local minimum of $[Br^-]$ its velocity slows to that of the first wave. Figure 34 shows the $[Br^-]$ at three different times. The second wave approaches the non-monotonic wake of the first, and quickly catches up before slowing.

3.5.2 Multiple Chemical Waves Displaying Anomalous Velocity Dispersion

Figure 35 shows conditions where multiple perturbations have been applied to a system near to the steady state. It must be mentioned that the initial value of [Q] has been modified to provide additional stability to the system. Temporally uniform perturbations were applied, creating eight spatially non-uniform pulses. Pulses are

Figure 34: Multiple [Br^-] peaks in a Quasi One-Dimensional System

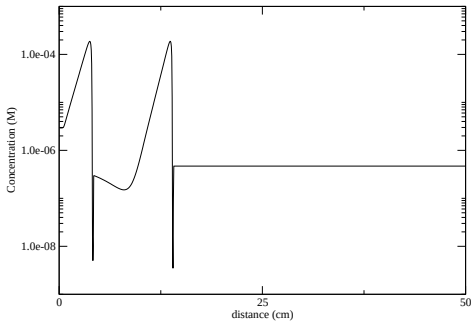

(a) t=50

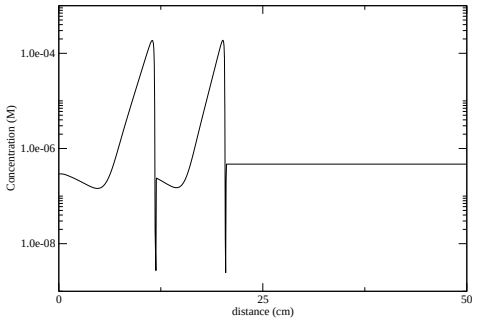

(b) t=150

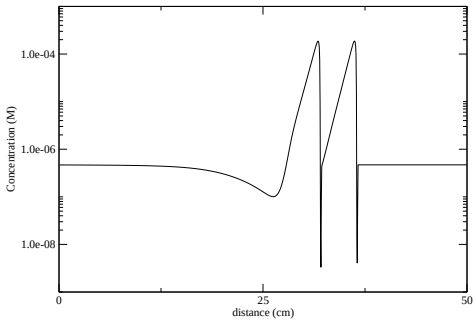

(c) t=400

A=0.06 M, B=0.02 M, H=0.5 M, g=0.2, f=2.1, $[Q]_0$=0.09 M. The initial interpulse distance is 11 cm.

Figure 35: Multiple Traveling Waves Exhibiting Anomalous Velocity Dispersion

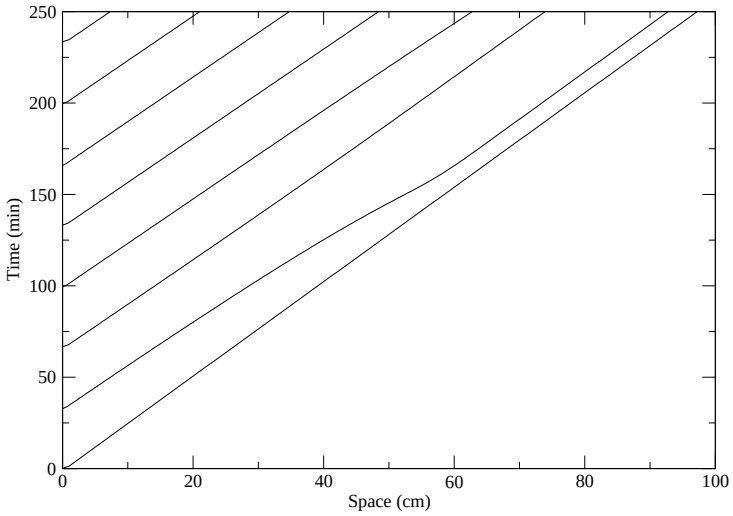

A=0.06 M, B=0.02 M, H=0.05 M, f=2.1, g=0.2 [Q_0]=0.0961 M. Perturbations are applied every 2000 s.

counted from the origin, increasing in number along the y-axis. The second pulse in the sequence travels at an increased velocity with relation to pulse one, and reaches the dip in [Br^-]. Upon reaching the first pulse there is no longer a decresed [Br^-], and the second pulse travels with identical velocity to pulse one. The temporally uniform perturbations result in the pulses formed having non-uniform spatial distribution. Pulses three through eight are near λ_{max}, and do not display anomalous velocity.

Figure 36 shows a calculation performed with identical paramater conditions to fig. 35. In this calculation the time between perturbations was decreased, thus the interpulse distance has also decreased. The behavior in fig. 36 has a striking resemblance to the behavior described by (Bordyugov et al. (2010)) as "wave bunching." The pulses in both experiment and calculation have a tendency to form pairs because of the non-uniform spatial distribution in the reaction medium.

Figure 36: Multiple Traveling Waves Exhibiting Anomalous Velocity Dispersion

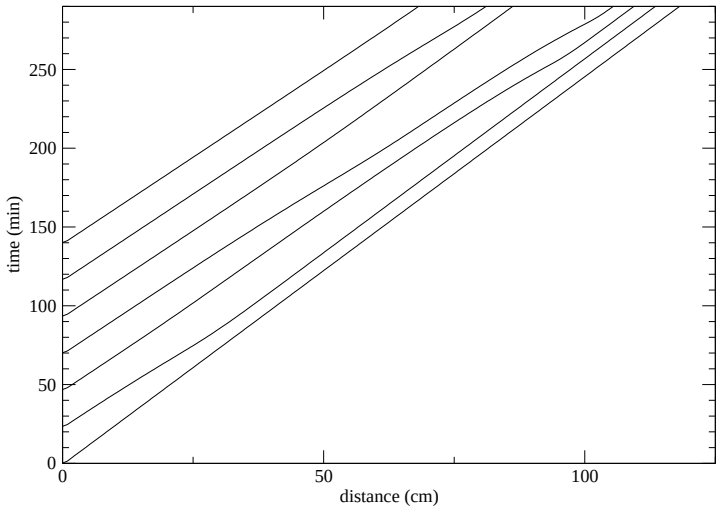

A=0.06 M, B=0.02 M, H=0.05 M, f=2.1, g=0.2, Q_0=0.0961 M

Figure 37: Space–time Trajectories of Fronts in a System with Bunching Dynamics

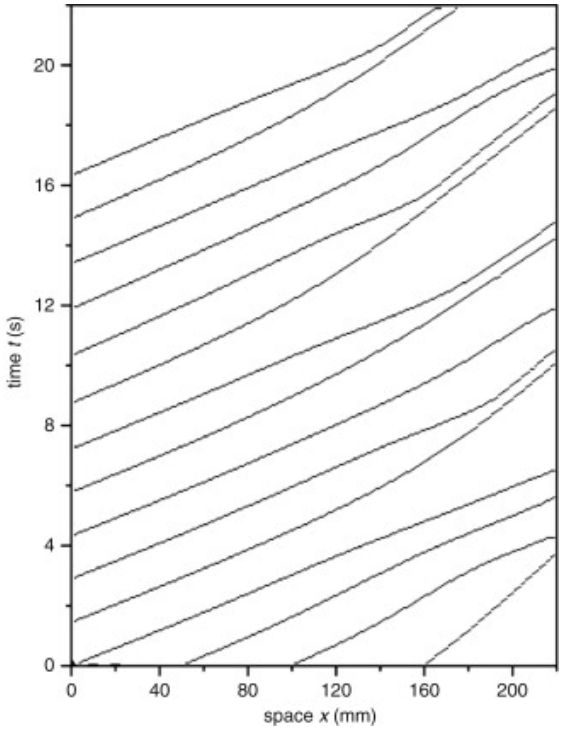

$[H_2SO_4]$=2.0 M, [CHD]=0.15 M, $[NaBrO_3]$=0.14 M. Figure from Bordyugov et al. (2010).

3.5.3 "Backfiring" and Stable Wave Trains

Steinbock and co-workers have observed a phenomena described as "backfiring" in experiments on the CHD-BZ system. This phenomenon arises in the six-variable spatially distributed model under a variety of parameter conditions. Backfiring is observed when the [Br^-] falls to the critical level in the dip behind a wave front, and Process B becomes dominant. Figure 38 is a time-space plot showing the emergence of a backfiring event at the tail end of a wavetrain. A second perturbation applied at a distance of 20.4 cm behind the first resulted in a multiple oscillatory excursion. The dip following the tenth pulse in the series initates Process B, and a new initiation point is formed, which undergoes a single oscillatory excursion. A time series of pulse formation is shown in figure 39. The line with negative slope in the upper left hand corner of figure 38 is a newly formed pulse traveling in the opposite direction. While backfiring pulses have been observed experimentally (Manz and Steinbock (2006)), the initation center has not been seen to form a new pulse traveling in the forward direction as well as the reverse, as is seen here. Initiation points spontaneously formed in the wake of traveling chemical waves may also undergo multiple oscillatory excursions.

3.6 Five-Variable Spatially Distributed System

The five-variable model reduction is also extended into a spatially distributed quasi one-dimensional system using Fick's second law of diffusion. The equations become:

$$\begin{aligned}
(\varepsilon)\tfrac{dx}{d\tau} &= \rho y - xy + x(1 - z/c0) - x^2 + \tfrac{\delta x}{\delta \tau}_{flux} \\
(\epsilon')\tfrac{dy}{d\tau} &= fz - xy - \rho y + \tfrac{\delta y}{\delta \tau}_{flux} \\
\tfrac{dz}{d\tau} &= x(1 - z/c0) - z + \tfrac{\delta z}{\delta \tau}_{flux} \\
(\chi)\tfrac{dj}{d\tau} &= gx(1 - z/C_0) - jm + \tfrac{\delta j}{\delta \tau}_{flux} \\
(\psi)\tfrac{dm}{d\tau} &= jm - p'm^2 + \tfrac{\delta m}{\delta \tau}_{flux}
\end{aligned} \tag{16}$$

Figure 38: Backfiring in an Unstable Wave Train

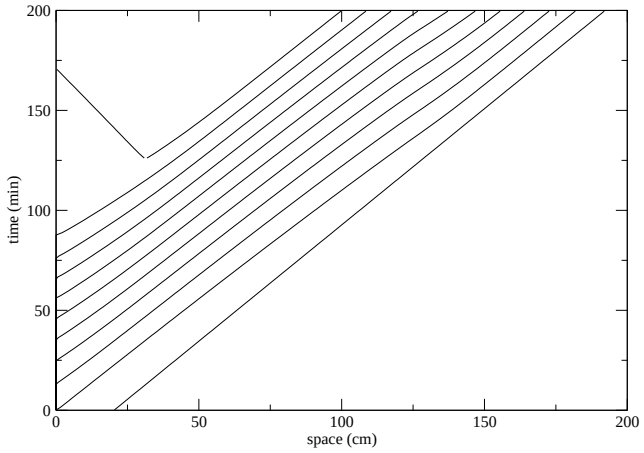

$A = 0.06$ M, $B = 0.02$ M, $H = 1.0$ M, $g = 0.2$, $f = 6.3$

The five-variable model fails to produce anomalous wave velocity dispersion. The figures 40 and 41 show calculations performed using the five-variable reduced model. While a non-monotonic recovery to the steady-state concentration is observed in j, this is not the inhibitor species in wave propagation. Consequently, conditions do not exist in the five-variable reduced model where anomalous velocity dispersion observed.

Figure 39: [Br^-] Time Series of "Backfiring"

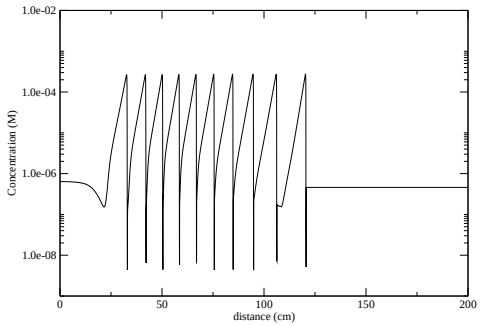

(a) t=7000 s

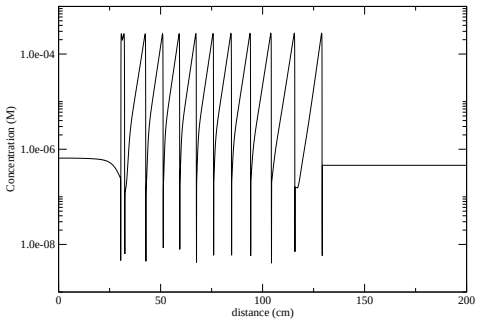

(b) t = 7600 s

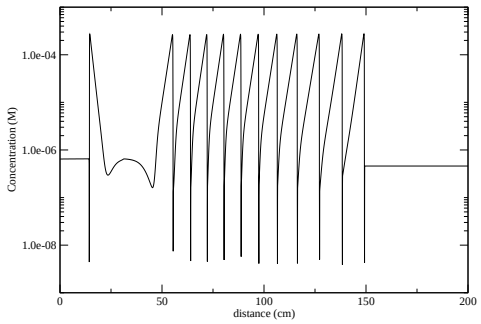

(c) t = 9000 s
$A = 0.06$ M, $B = 0.02$ M, $H = 1.0$ M, $g = 0.2$, $f = 6.3$

Figure 40: Five-Variable Spatially Distributed System

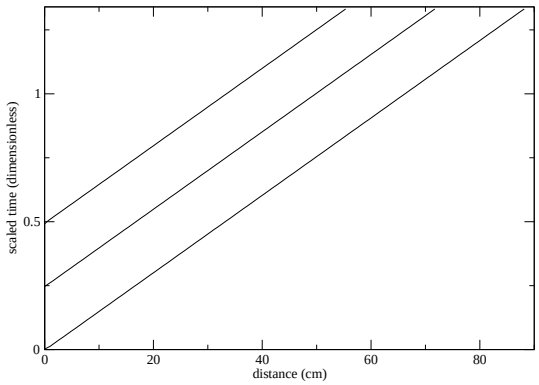

A=0.1 M, B=0.05, H=2.0 M, f=2.5, g=0.2. Pulses are applied at τ=0, 0.25, and 0.5 in scaled time.

Figure 41: Five-Variable Spatially Distributed System

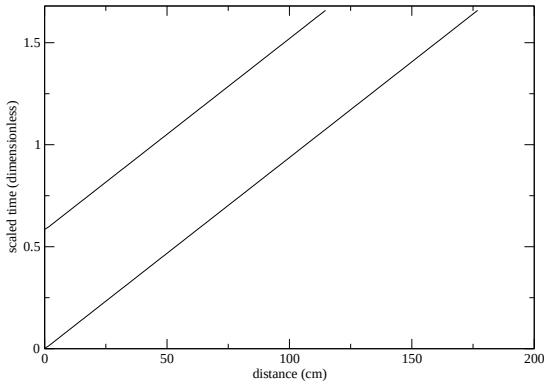

$A = 0.1$ M, $B = 0.05$ M, $H = 2.0$ M, $f = 2.5$, $g = 0.2$. Perturbations are applied at $\tau = 0$ and 0.6 in scaled time.

4 Conclusions and Future Direction

The modified six-variable Oregonator model presented here successfully reproduces a significant amount of the experimental behavior observed in the CHD-BZ system. The phenomena of anomalous velocity dispersion, wave-stacking, and backfiring have been successfully reproduced numerically in terms of a non-montonic [Br^-] decay to the steady state in the wake of an excitation pulse. The origin of anomalous dispersion as the result of such a non-monotonic decay curve in [Br^-] has been suggested previously by Steinbock et. el, Szalai et. el, as a precondition for anomalous dispersion. However, the work presented here is the first successful representation of anomalous dispersion using a chemical model. This model is based on the well-understood chemistry of the Oregonator model of the Belousov-Zhabotinsky reaction, coupled to a second pathway (based on chemistry related to uncatalyzed bromate oscillators) for the oxidation of organic substrate to provide the new dynamics.

We believe that future work in this area should begin with re-evaluation of the mechanism based upon what has been learned with the modified Oregonator model presented here, and recent new experimental results (Jichan Wang, private communication). Potential unification of this model with the five-variable skeleton model presented by Szalai et al. should also be pursued. While the Szalai model does not produce non-montonic decay in [Br^-] to the steady state, it provides an experimentally based mechanism for a second oxidation pathway of the organic substrate. It is possible that this chemistry can provide insight into the identities of intermediate species in the CHD-BZ system.

The effect of Parameters A, B, H, and f on wave velocity is also a potential area for exploration. These parameters play an important role in the stability of the modified Oregonator model. It is reasonable to explore their impact on the [Br^-] steady state, and resulting effect on wave velocity. Exploration of diffusion effects on the waveforms as well as the role of [Br^-] on wave velocity is also a potential area of

interest.

References

Atkins, P. and de Paula, J. (2009). Physical chemistry. *Oxford University Press, New York*.

Babu, J. and Srinivasulu, K. (1976). Cobalt ion catalyzed self-oscillatory reaction in closed system of potassium bromate and gallic acid. *Proc. Indian Natl. Sci. Acad., Part A*, 42(5):361-3. CAPLUS AN 1977:444773(Journal).

Belousov, B. (1982). The oscillating reaction and its mechanism. *Khim. Zhizn*, (7):65-8. CAPLUS AN 1982:526531(Journal; General Review).

Belousov, B. P. (1958). A periodic reaction and its mechanism. *Sbornik Referatov po Radiatsionni Meditsine*, 145.

Bordyugov, G., Fischer, N., Engel, H., Manz, N., and Steinbock, O. (2010). Anomalous dispersion in the belousov-zhabotinsky reaction: Experiments and modeling. *Physica D*, 239(11):766-775.

Boyle, R. (1680). Experiments and observations made upon the icy noctiluca.

Bray, W. (1921). Periodic reaction in homogeneous solution and its relation to catalysis. *Journal of the american chemical society*, 43:1262-7. CAPLUS AN 1921:20916(Journal).

Bray, W. and Caulkins, A. (1931). Reactions involving hydrogen peroxide, iodine and iodate ion. ii. the preparation of iodic acid. preliminary rate measurements. *Journal of the american chemical society*, 53:44-8. CAPLUS AN 1931:13298(Journal).

Bray, W. and Liebhafsky, H. (1931). Reactions involving hydrogen peroxide, iodine and iodate ion. i. introduction. *Journal of the american chemical society*, 53:38-44. CAPLUS AN 1931:13297(Journal).

Britton, M. (2003). Nuclear magnetic resonance studies of the 1, 4-cyclohexanedione-bromate-acid oscillatory system. *J. Phys. Chem. A*.

Epstein, I. and Pojman, J. (1998). *An Introduction to Nonlinear Chemical Dynamics: Oscillations, Waves, Patterns, and Chaos.* CAPLUS AN 1999:137882(Book).

Epstein, I. R., Pojman, J., and Steinbock, O. (2006). Introduction: Self-organization in nonequilibrium chemical systems. *Chaos*, 16.

Espenson, J. H. (1995). Chemical kinetics and reaction mechanisms. *McGraw-Hill*.

Farage, V. and Janjic, D. (1982a). Uncatalyzed oscillatory chemical reaction. oxidation of 1,4-cyclohexanedione by bromate in sulfuric or nitric acid solution. *Chemical Physics Letters*, 88(3):301-4. CAPLUS AN 1982:423090(Journal).

Farage, V. and Janjic, D. (1982b). Uncatalyzed oscillatory chemical reactions. effect of different constraints during the oxidation reaction of 1,4-cyclohexanedione by acidic bromate. *Chemical Physics Letters*, 93(6):621-4. CAPLUS AN 1983:88641(Journal).

Fechner, A. T. (1828). Ueber umkehrungen der polaritaet der einfachen kette. *Schweigg, J.*, 53:61-77.

Field, R. and Foersterling, H. (1986). On the oxybromine chemistry rate constants with cerium ions in the field-koeroes-noyes mechanism of the belousov-zhabotinskii reaction. *Journal of Physical Chemistry*, 90(21):5400-7. CAPLUS AN 1986:559496(Journal).

Field, R. and Noyes, R. (1974a). Oscillations in chemical systems. iv. limit cycle behavior in a model of a real chemical reaction. *J. Chem. Phys.*, 60(5):1877-84. CAPLUS AN 1974:417165(Journal).

Field, R. and Noyes, R. (1974b). Oscillations in chemical systems. v. quantitative explanation of band migration in the belousov-zhabotinskii reaction. *Journal of the american chemical society*, 96(7):2001-6. CAPLUS AN 1974:430133(Journal).

Field, R. and Troy, W. (1979). The existence of solitary traveling wave solutions of a model of the belousov-zhabotinskii reaction. *SIAM Journal on Applied Mathematics*, 37(3):561-587.

Field, R. J. (2008). Chemical reaction kinetics. *Scholarpedia*, 3(10):4051.

Field, R. J., Koros, E., and Noyes, R. M. (1972). Oscillations in chemical systems. ii. thorough analysis of temporal oscillation in the bromate-cerium-malonic acid system. *Journal of the american chemical society*, 94(25):8649-8664.

Freire, J. G., Field, R. J., and Gallas, J. A. C. (2009). Relative abundance and structure of chaotic behavior: The nonpolynomial belousov-zhabotinsky reaction kinetics. *J. Chem. Phys.*, 131(4):044105.

Ginn, B. T. and Steinbock, O. (2005). Front aggregation in multiarmed excitation vortices. *Phys. Rev. E*, 72.

Gray, P., Scott, S., and Showalter, K. (1991). The influence of the form of autocatalysis on the speed of chemical waves. *Philos. Trans. R. Soc. London, Ser. A*, 337(1646):249-60. CAPLUS AN 1992:159801(Journal).

Gray, P. and Scott, S. K. (1990). Chemical oscillations and instabilities-nonlinear chemical kinetics. *Oxford Science Publications, Oxford University Press, Oxford.*

Gyorgyi, L. and Field, R. (1992). Simulation of the effect of stirring rate on bistability in the bromate-cerium(iii)-bromide cstr reaction. *Journal of Physical Chemistry*, 96(3):1220-4. CAPLUS AN 1992:92294(Journal).

Gyorgyi, L., Field, R., Noszticzius, Z., McCormick, W., and Swinney, H. (1992). Confirmation of high flow rate chaos in the belousov-zhabotinskii reaction. *Journal of Physical Chemistry*, 96(3):1228-33. CAPLUS AN 1992:92295(Journal).

Gyorgyi, L. and Field, R. J. (1991). Simple models of deterministic chaos in the belousov-zhabotinskii reaction. *J. Phys. Chem.*, 95:6594-6602.

Gyorgyi, L., Turanyi, T., and Field, R. J. (1990). Mechanistic details of the oscillatory belousov-zhabotinskii reaction. *J. Phys. Chem.*, 94(18):7162-7170.

Hamik, C. T. and Steinbock, O. (2003). Excitation waves in reaction-diffusion media with non-monotonic dispersion relations. *New Journal of Physics*, 5:58.1-58.12.

Hastings, H., Field, R. J., and Sobel, S. G. (2003). Microscopic fluctuations and pattern formation in a supercritical oscillatory chemical system. *J. Chem. Phys.*, 119.

Hegedus, L., Wittmann, M., Noszticzius, Z., Yan, S., Sirimungkala, A., Foersterling, H.-D., and Field, R. (2001). Hplc analysis of complete bz systems. evolution of the chemical composition in cerium and ferroin catalysed batch oscillators: experiments and model calculations. *Faraday Discuss.*, 120:21-38. CAPLUS AN 2002:61289(Journal).

Hindmarsh, A. C. (1980). Lsode and lsodi, two new initial value ordinary differnetial equation solvers. *SIGNUM Newsl.*, 15:10-11.

Houston, P. L. (2001). Chemical kinetics and reaction dynamics. *McGraw-Hill*.

Huh, D., Choe, S., and Kim, M. (2001). The revival wave induced spontaneously in a bz-type mixture. *Reaction Kinetics and Catalysis Letters*, 74(1):11-22.

Janz, R. D., Vanecek, D., and Field, R. (1980). Composite double oscillation in a modified version of the oregonator model of the belousov-zhabotinsky reaction. *J. Chem. Phys.*, 73(7):3132-3138.

Kalachev, L. and Field, R. (2001). Reduction of a model describing ozone oscillations in the troposphere: example of an algorithmic approach to model reduction in atmospheric chemistry. *J. Atmos. Chem.*, 39(1):65-93. CAPLUS AN 2001:411895(Journal).

Koros, E., Szalai, I., Kurin-Csorgei, K., and Nagy, G. (1998). A novel type of bromate oscillator: The 1,4-cyclohexanedione-bromate-acid system. *Phys. Chem. '98, Int. Conf. Fundam. Appl. Aspects Phys. Chem., 4th*, pages 183-185. CAPLUS AN 1999:39463(Conference).

Kuhnert, L. and Linde, H. (1977). The reaction of diazonium salt with bromate, a new oscillating reaction in

homogeneous phase. *Z. Chem.*, 17(1):19-20. CAPLUS AN 1977:188806(Journal).

Lefever, R., Nicolis, G., and Prigogine, I. (1967). On the occurrence of oscillations around the steady state in systems of chemical reactions far from equilibrium. *J. Chem. Phys.*, 47(3):1045-6. CAPLUS AN 1967:485018(Journal).

Liebhafsky, H., Furuichi, R., and Roe, G. (1981). Reactions involving hydrogen peroxide, iodine, and iodate ion. 7. the smooth catalytic decomposition of hydrogen peroxide, mainly at 50â°c. *Journal of the american chemical society*, 103(1):51-6. CAPLUS AN 1981:72194(Journal).

Lotka, A. (1910). Contribution to the theory of periodic reactions. *J. Phys. Chem.*, 14(3):271-274.

Lotka, A. (1920). Undamped oscillations derived from the law of mass action. *Journal of the american chemical society*, 42(8):1595-1599.

Manz, N., Ginn, B., and Steinbock, O. (2006). Propagation failure dynamics of wave trains in excitable systems. *Phys. Rev. E*, 73.

Manz, N. and Steinbock, O. (2004). Tracking waves and spiral drift in reaction - diffusion systems with finite bandwidth dispersion relations. *J. Phys. Chem. A*, 108(25).

Manz, N. and Steinbock, O. (2006). Propagation failures, breathing pulses, and backfiring in an excitable reaction-diffusion system. *Chaos*, 16.

Maselko, J. and Swinney, H. (1986). Complex periodic oscillations and farey arithmetic in the belousov-zhabotinskii reaction. *J. Chem. Phys.*, 85(11):6430-41. CAPLUS AN 1987:39163(Journal).

Nicolis, G. and Prigogine, I. (1977). *Self-Organization in Nonequilibrium Systems: From Dissipative Structures to Order Through Fluctuations*. CAPLUS AN 1978:55278(Book).

Nicolis, G. and Prigogine, I. (1989). Exploring complexity. *W.H. Freeman and Complany*.

Nicolis, G., Prigogine, I., and Glansdorff, P. (1975). On the mechanism of instabilities in nonlinear systems. *Adv. Chem. Phys.*, 32(Proc. Conf. Instab. Dissipative Struct. Hydrodyn., 1973):1-11. CAPLUS AN 1976:437333(Journal; General Review).

Noyes, R., Field, R., and Thompson, R. (1971). Mechanism of reaction of bromine(v) with weak one-electron reducing agents. *Journal of the american chemical society*, 93(26):7315-16. CAPLUS AN 1972:50563(Journal).

Orban, M. and Koros, E. (1978a). Chemical oscillations during the uncatalyzed reaction of aromatic compounds with bromate. 1. search for chemical oscillators. *Journal of Physical Chemistry*, 82(14):1672-5. CAPLUS AN 1978:475287(Journal).

Orban, M. and Koros, E. (1978b). Novel type of oscillatory

chemical reactions. *Reaction Kinetics and Catalysis Letters*, 8(2):273-6. CAPLUS AN 1978:495668(Journal).

Ostwald, W. (1899). Periodisch veraend reaktiongeschwindigkeiten. *Phys. Zeitsch.*, 8:87-88.

Pitzer, K. S. (1995). Thermodynamics. *McGraw-Hill*.

Prigogine, I. and Nicolis, G. (1967). Symmetry-breaking instabilities in dissipative systems. *J. Chem. Phys.*, 46(9):3542-50. CAPLUS AN 1967:413221(Journal).

Roux, J., Simoyi, R., and Swinney, H. (1983). Observation of a strange attractor. *Physica D*, 8D(1-2):257-66. CAPLUS AN 1983:564649(Journal).

Scott, S. K. (1994). Oscillations, waves and chaos in chemical kinetics. *Oxford Science Publications, Oxford University Press, Oxford*.

Steinfeld, J., Francisco, J., and Hase, W. (1999). *Chemical Kinetics Dynamics, Second Edition.* CAPLUS AN 2000:676614(Book).

Strogatz, S. H. (2001). *Nonlinear Dynamics and Chaos:With Applications to Physics, Biology, Chemistry, and Engineering*.

Szalai, I., Kurin-Csoergei, K., Epstein, I., and Orban, M. (2003). Dynamics and mechanism of bromate oscillators with 1,4-cyclohexanedione. *J. Phys. Chem. A*, 107(47):10074-10081. CAPLUS AN 2003:851630(Journal).

Szalai, I., Kurin-Csoergei, K., and Orban, M. (2002). Mechanistic studies on the bromate-1,4-cyclohexanedione-ferroin oscillatory system. *Phys. Chem. Chem. Phys.*, 4(8):1271-1275. CAPLUS AN 2002:252816(Journal).

Thompson, R. (1971). Reduction of bromine(v) by cerium(iii), manganese(ii), and neptunium(v) in aqueous sulfuric acid. *Journal of the american chemical society*, 93(26):7315. CAPLUS AN 1972:50564(Journal).

Tinsley, M. and Field, R. (2001). Steady state instability and oscillation in simplified models of tropospheric chemistry. *J. Phys. Chem. A*, 105(50):11212-11219. CAPLUS AN 2001:833987(Journal).

Turing, A. (1952). The chemical basis of morphogenesis. *Philosophical Transactions of the Royal Society of London B*, 237:37-72.

Tyson, J. (1973). Nonlinear oscillations in chemical systems. *J. Chem. Phys.*, 58(9):3919-30. CAPLUS AN 1973:164776(Journal).

Tyson, J., Alexander, K., Manoranjan, V., and Murray, J. (1989). Spiral waves of cyclic amp in a model of slime mold aggregation. *Physica D*, 34(1-2):193-207. CAPLUS AN 1989:189177(Journal).

Tyson, J. and Light, J. (1973). Properties of two-component

bimolecular and trimolecular chemical reaction systems. *J. Chem. Phys.*, 59(8):4164-73. CAPLUS AN 1974:52715(Journal).

Tyson, J. J. (1982). Scaling and reducing the field-koros-noyes mechanism of the belousov-zhabotinskii reaction. *J. Phys. Chem.*, 86(15):3006-3012.

Vanag, V. and Epstein, I. (2001). Pattern formation in a tunable medium: the belousov-zhabotinskii reaction in an aerosol ot microemulsion. *Physical review letters*, 87(22):228301/1-228301/4. CAPLUS AN 2001:838471(Journal).

Vanag, V. and Epstein, I. (2002). Comparative analysis of packet and trigger waves originating from a finite wavelength instability. *J. Phys. Chem. A*, 106(46):11394-11399. CAPLUS AN 2002:799311(Journal).

Winfree, A. (1972). Spiral waves of chemical activity. *Science (Washington, DC, U. S.)*, 175(4022):634-6. CAPLUS AN 1972:104343(Journal).

Winfree, A. (2002). Oscillating systems: On emerging coherence. *Science (Washington, DC, U. S.)*, 298(5602):2336-2337. CAPLUS AN 2002:982601(Journal; General Review).

Yang, L., Dolnik, M., Zhabotinsky, A., and Epstein, I. (2002). Pattern formation arising from interactions between turing and wave instabilities. *J. Chem. Phys.*, 117:7259.

Zaikin, A. and Zhabotinskii, A. (1970). Concentration wave propagation in two-dimensional liquid-phase self-oscillating system. *Nature (London)*, 225(5232):535-7. CAPLUS AN 1970:104329(Journal).

Zhabotinsky, A. (1991). A history of chemical oscillations and waves. *Chaos*, 1(4):379-386.